Tuning Vibration-Induced Emission through Macrocyclization and Catenation

Wei-Tao Xu,[a] Zhiyong Peng,[a] Peicong Wu,[b] Yefei Jiang,[a] Wei-Jian Li,[a] Xu-Qing Wang,[a] Jinquan Chen,[b] Hai-Bo Yang [ac] and Wei Wang *[a]

[a]Shanghai Key Laboratory of Green Chemistry and Chemical Processes, State Key Laboratory of Petroleum Molecular and Process Engineering (SKLPMPE), School of Chemistry and Molecular Engineering, East China Normal University, 3663 N. Zhongshan Road, Shanghai 200062, China.

[b]State Key Laboratory of Precision Spectroscopy, School of Physics and Electronic Science, East China Normal University, Dongchuan Road 500, Shanghai 200241, China.

[c]Shanghai Center of Brain-inspired Intelligent Materials and Devices, East China Normal University, Shanghai 200241, China.

* Corresponding authors.

E-mail: wwang@chem.ecnu.edu.cn (W. W.)

Table of contents

Section A. Materials and general methods.

All reagents were commercially available and used as supplied without further purification, compounds **S1**, DEP[5]A, and dumbbell **3** were prepared according to the published.[S1-S3] Deuterated solvents were purchased from Cambridge Isotope Laboratory (Andover, MA).

All solvents were dried according to standard procedures and all of them were degassed under N_2 for 30 minutes before use. All air-sensitive reactions were carried out under inert N_2 atmosphere. ^{1}H NMR and ^{13}C NMR spectra were recorded on Bruker 400 MHz Spectrometer (^{1}H: 400 MHz; ^{13}C: 101 MHz) and Bruker 500 MHz Spectrometer (^{1}H: 500 MHz; ^{13}C: 126 MHz) at 298 K. ^{19}F NMR spectra were recorded on Bruker 400 MHz Spectrometer (^{19}F: 376 MHz) at 298 K. The ^{1}H and ^{13}C NMR chemical shifts are reported relative to residual solvent signals. 2D-NMR spectra (NOESY, DOSY) were recorded on Bruker 400 MHz Spectrometer (^{1}H: 400 MHz) and Bruker 500 MHz Spectrometer (^{1}H: 500 MHz) 298 K. The high resolution electron spray ionization mass spectra (HR ESI-MS) were performed on an Agilent (Santa Clara, CA, USA) ESI-TOF mass spectrometer (6224) and micrOTOF mass spectrometer.

UV-vis spectra and fluorescence spectra were recorded in a quartz cell (light path 1 cm) on a Shimadzu UV2700 UV-visible spectrophotometer and a Shimadzu RF-6000 fluorescence spectrophotometer respectively. Femtosecond transient absorption (TA) spectra was measured using TA spectrometer (Helios-EOS fire, Ultrafast System). All experiments were carried out at room temperature and a 2 mm fused silica cuvette was used in TA experiments. The fundamental pulses were generated with a Ti: sapphire laser system (Astrella, 360 nm, 100 fs, 7 mJ/pulse, and 1 kHz repetition rate, Coherent Inc.). White light continuum (WLC) probe beam was generated by focusing the fundamental beam into a CaF_2 or YaG and the time window limit is ~7.6 ns. A fraction of the fundamental beam was used to produce pump beams via an optical parametric amplifier (OPerA Solo, Coherent Inc.). The instrument response function (IRF) of this

system was determined to be ~120 fs by measuring solvent responses under the same experimental conditions.

Chiral resolution was performed using a Shimadzu HPLC System (LC-20AR) equipped with a CHIRALPAK IC® column (250 mm L × 10 mm I. D. for separation and 250 mm L × 4.6 mm I. D. for analysis) and eluting with hexane/dichloromethane at flow rates of 3.0 mL/min for separation and 1.0 mL/min for analysis. Circular dichroism (CD) and Circularly Polarized Luminescence (CPL) spectra were measured on a Chirascan Series Spectrometer (Applied Photophysics Ltd, UK) at room temperature. The solid CPL sample were prepared in KBr pellet at a sample concentration of 2% (w/w) using the same procedure that used for IR measurements, and had a diameter of 10 mm. The excitation wavelength was 340 nm, and the emission bandwidth was 10 nm.

Section B. Synthesis and characterization of macrocycle **DPAC-M** and [2]catenane **DPAC-C**.

Scheme S1. The synthetic route of macrocycle **DPAC-M** and [2]catenane **DPAC-C**.

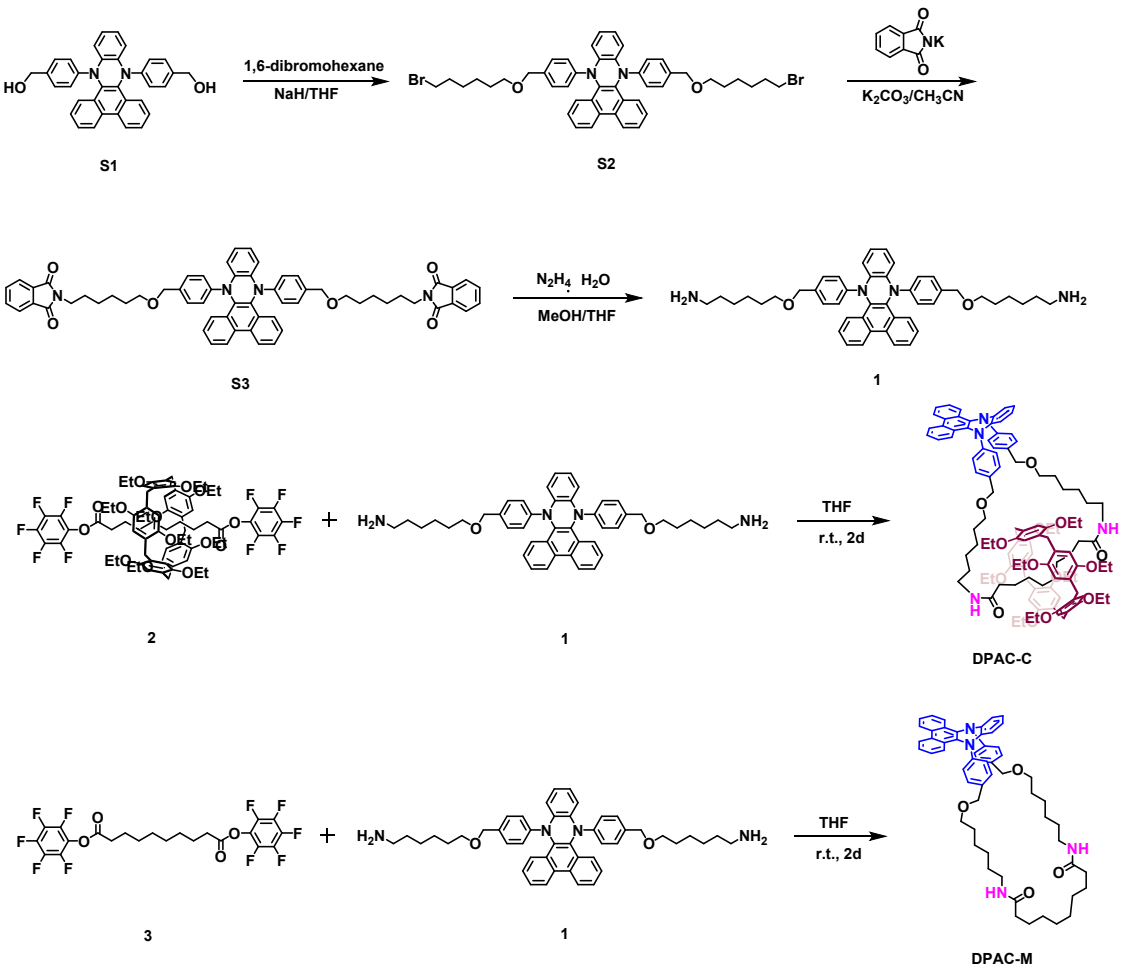

Synthesis of compound S2: A Schlenk flask was charged with **S1** (1.13 g, 2.28 mmol) and NaH (0.35 g, 9.11 mmol). The Schlenk flask was then evacuated and back-filled with N_2 three times. Next, the solvent of degassed THF (100 mL) was added via syringe at 0 °C. Then, 1,6-dibromohexane (3.33 g, 13.67 mmol) was added. The reaction was heated to 75 °C and stirred for 12 h. After cooling to room temperature, the reaction mixture was filtered and the filtrate was concentrated in vacuum. The resultant residue was purified by column chromatography (SiO_2: PE/DCM 1:1) to obtain 0.64 g white solid with the yield of 34.1%. ^{1}H NMR (500 MHz, CD_2Cl_2) δ 8.78-8.76 (d, J = 10.0

Hz, 2H), 8.09-8.07 (d, *J* = 10.0 Hz, 2H), 7.79-7.77 (m, 2H), 7.68-7.65 (t, *J* = 15.0 Hz, 2H), 7.57-7.54 (d, *J* = 15.0 Hz, 2H), 7.38-7.36 (m, 2H), 7.02-6.96 (m, 8H), 4.27 (s, 4H), 3.40-3.35 (m, 8H), 1.85-1.79 (m, 4H), 1.56-1.51 (m, 4H), 1.43-1.31 (m, 8H). ^{13}C NMR (126 MHz, CD_2Cl_2) δ 147.48, 145.09, 138.29, 132.10, 130.41, 129.69, 128.86, 127.66, 127.37, 127.00, 125.86, 124.86, 123.52, 117.05, 72.74, 70.59, 34.49, 33.27, 30.01, 28.43, 25.84. HRMS (ESI-TOF): Calculated for [**S2** + NH_4]$^+$ ($C_{46}H_{52}Br_2N_3O_2$): 838.2406; Found: 838.2396.

Synthesis of compound S3: Mixing compound **S2** (500 mg, 0.63 mmol) and potassium phthalimide (467 mg, 2.52 mmol) in acetonitrile (pre-dried by Na_2SO_4, 100 mL), then K_2CO_3 (348 mg, 2.52 mmol) was added into the reaction flask. The resultant suspension was refluxed at 88 °C overnight. After cooling to room temperature, the reaction mixture was filtered and the filtrate was concentrated in vacuum. The resultant residue was purified by column chromatography (SiO_2: PE/EA 5:1) to obtain 469 mg white solid with the yield of 80.3%. ^{1}H NMR (500 MHz, CD_2Cl_2) δ 8.76-8.74 (d, *J* = 10.0 Hz, 2H), 8.08-8.06 (d, *J* = 10.0 Hz, 2H), 7.80-7.76 (m, 6H), 7.72-7.69 (m, 4H), 7.67-7.64 (t, *J* = 15.0 Hz, 2H), 7.56-7.53 (t, *J* = 10.0 Hz, 2H), 7.37-7.35 (m, 2H), 7.01-6.96 (m, 8H), 4.25 (s, 4H), 3.63-3.60 (t, *J* = 15.0 Hz, 4H), 3.36-3.33 (t, *J* = 15.0 Hz, 4H), 1.64-1.60 (m, 4H), 1.51-1.50 (m, 4H), 1.34-1.30 (m, 4H). ^{13}C NMR (126 MHz, CD_2Cl_2) δ 168.71, 147.46, 145.11, 138.30, 134.22, 132.74, 132.16, 130.40, 129.70, 128.87, 127.63, 127.36, 126.97, 125.83, 124.88, 123.49, 123.34, 117.09, 72.70, 70.64, 38.32, 30.04, 28.93, 27.13, 26.25. HRMS (ESI-TOF): Calculated for [**S3** + Na]$^+$ ($C_{62}H_{56}N_4NaO_6$): 975.4098; Found: 975.4087.

Synthesis of compound 1: Compound **S3** (400 mg, 0.42 mmol) was added in a Schlenk flask, after the Schlenk flask was evacuated and back-filled with N_2 three times, the mixture solvent of THF (50 mL) and MeOH (12.5 mL) were added via syringe, then hydrazine hydrate (1.2 mL) was added under an inert atmosphere. The reaction was heated to 66 °C and stirred for 12 h. After cooling to room temperature, the reaction mixture was filtered and the filtrate was concentrated in vacuum. The obtained residue was washed by sodium hydroxide aqueous solution, then dried with Na_2SO_4 and concentrated to obtain 266 mg white solid with the yield of 95.5%. ^{1}H NMR (300 MHz,

CD_2Cl_2) δ 8.78-8.75 (d, *J* = 9.0 Hz, 2H), 8.09-8.06 (m, 2H), 7.79-7.76 (m, 2H), 7.70-7.64 (m, 2H), 7.58-7.53 (m, 2H), 7.39-7.35 (m, 2H), 7.03-6.95 (m, 8H), 4.26 (s, 4H), 3.38-3.34 (t, *J* = 12.0 Hz, 4H), 2.62-2.57 (t, *J* = 15.0 Hz, 4H), 1.55-1.48 (m, 4H), 1.41-1.27 (m, 12H). ^{13}C NMR (126 MHz, CD_2Cl_2) δ 147.39, 145.03, 138.24, 132.08, 130.35, 129.63, 128.84, 127.64, 127.34, 126.97, 125.82, 124.82, 123.48, 116.95, 72.67, 70.74, 42.60, 34.33, 30.16, 27.13, 26.50. HRMS (ESI-TOF): [**1** + H]$^+$ ($C_{46}H_{53}N_4O_2$): 693.4169; Found: 693.4153.

Synthesis of [2]rotaxane 2: A Schlenk flask was charged with sebacyl chloride (0.47 g, 2.0 mmol), DEP[5]A (4.7 g, 5.0 mmol). The Schlenk flask was then evacuated and back-filled with N_2 three times. Next, 10 mL of the freshly distilled $CHCl_3$ was added via syringe. The resultant solution was stirred for 1 h under -15 °C. Then the mixture of pentafluorophenol (0.81 g, 4.4 mmol) and Et_3N (0.53 g, 5.0 mmol) in 3 mL freshly distilled $CHCl_3$ was added to the solution under an inert atmosphere and the reaction mixture was allowed to warm to room temperature and stirred overnight. The solution was concentrated and the residue was purified by column chromatography (SiO_2; PE/DCM = 4:1, v/v) to obtain the white solid 1.8 g with the yield of 72%. ^{1}H NMR ($CDCl_3$, 500 MHz): *δ* = 6.92 (s, 10 H), 4.04-3.79 (m, 20 H), 3.76 (s, 10 H), 2.20-2.15 (m, 4 H), 1.46-1.24 (m, 38 H), 0.69-0.59 (m, 4 H), -0.91 (brs, 4 H), -1.42 (brs, 4 H); ^{19}F NMR ($CDCl_3$, 376 MHz): *δ* = -153.59, -157.95, -162.64; ^{13}C NMR (126 MHz, $CDCl_3$, 298 K): *δ* = 170.00, 149.81, 128.59, 114.43, 63.69, 33.13, 31.59, 30.36, 29.32, 27.75, 27.60, 24.94, 15.47, 1.17, 0.14; HRMS (ESI-TOF): Calcd. For [**2** + H]$^+$ ($C_{77}H_{86}F_{10}O_{14}$): 1424.5858, Found: 1424.5858.

Synthesis of macrocycle DPAC-M: Mixing dumbbell **3** (36 mg, 0.07 mmol) and compound **1** (47 mg, 0.007 mmol) in THF (pre-dried by Na_2SO_4, 500 mL), and the reaction mixture was stirred at room temperature for 48 h. The solution was concentrated and the residue was purified by column chromatography (SiO_2: EA) and preparative gel permeation chromatography (GPC) to obtain 19 mg white solid with the yield of 31.9%. ^{1}H NMR (500 MHz, CD_2Cl_2) *δ* 8.78-8.76 (d, *J* = 10.0 Hz, 2H), 8.10-8.08 (m, 2H), 7.78-7.76 (m, 2H), 7.68-7.65 (m, 2H), 7.57-7.54 (t, *J* = 15.0 Hz, 2H),

7.38-7.36 (m, 2H), 7.01-6.95 (m, 8H), 5.60-5.57 (t, J = 15.0 Hz, 2H), 4.28 (s, 4H), , 3.34-3.31 (t, J = 15.0 Hz, 4H), 3.16-3.12 (m, 4H), 2.08-2.05 (t, J = 15.0 Hz, 4H), 1.57-1.47 (m, 8H),, 1.44-1.39 (m, 4H), 1.29-1.25 (m, 16H). ^{13}C NMR (126 MHz, CD_2Cl_2) δ 173.08, 147.51, 145.11, 138.31, 132.05, 130.33, 129.65, 128.73, 127.62, 127.34, 126.97, 125.85, 124.77, 123.48, 117.10, 72.56, 70.47, 39.51, 36.89, 31.54, 30.36, 30.09, 29.96, 29.93, 28.90, 27.01, 26.28, 25.86. HRMS (ESI-TOF): [**DPAC-M** + H]$^+$ ($C_{56}H_{67}N_4O_4$): 859.5162; Found: 859.5127.

Synthesis of [2]catenane DPAC-C: Mixing [2]rotaxane **2** (108 mg, 0.08 mmol) and compound **1** (53 mg, 0.008 mmol) in THF (pre-dried by Na_2SO_4, 500 mL), and the reaction mixture was stirred at room temperature for 48 h. The solution was concentrated and the residue was purified by column chromatography (SiO_2: EA) and preparative gel permeation chromatography (GPC) to obtain 36 mg white solid with the yield of 27.1%. ^{1}H NMR (500 MHz, CD_2Cl_2) δ 8.79-8.77 (d, J = 10.0 Hz, 2H), 8.05-8.03 (m, 2H), 7.84-7.81 (m, 2H), 7.69-7.66 (m, 2H), 7.57-7.54 (t, J = 15.0 Hz, 2H), 7.42-7.38 (m, 2H), 7.08-7.02 (m, 8H), 6.78 (s, 10H), 5.14 (s, 2H), 4.23-4.21 (m, 2H), 3.83-3.66 (m, 30H), 2.86 (br, 4H), 2.65-2.25 (br, 4H), 2.12-2.09 (t, J = 15.0 Hz, 4H), 1.43-1.25 (m, 46H), 0.80-0.40 (br, 4H), 0.25-0.81(br, 4H).^{13}C NMR (126 MHz, CD_2Cl_2) δ 150.00, 146.78, 144.71, 137.85, 132.34, 130.41, 129.49, 128.68, 128.44, 127.56, 127.24, 126.93, 125.69, 124.92, 123.54, 116.63, 114.69, 72.67, 71.74, 64.09, 39.92, 36.83, 30.10, 29.71, 29.41, 29.38, 29.29, 26.00, 15.59. HRMS (ESI-TOF): [**DPAC-C** + H]$^+$ ($C_{111}H_{137}N_4O_{14}$): 1751.0165; Found: 1751.0162.

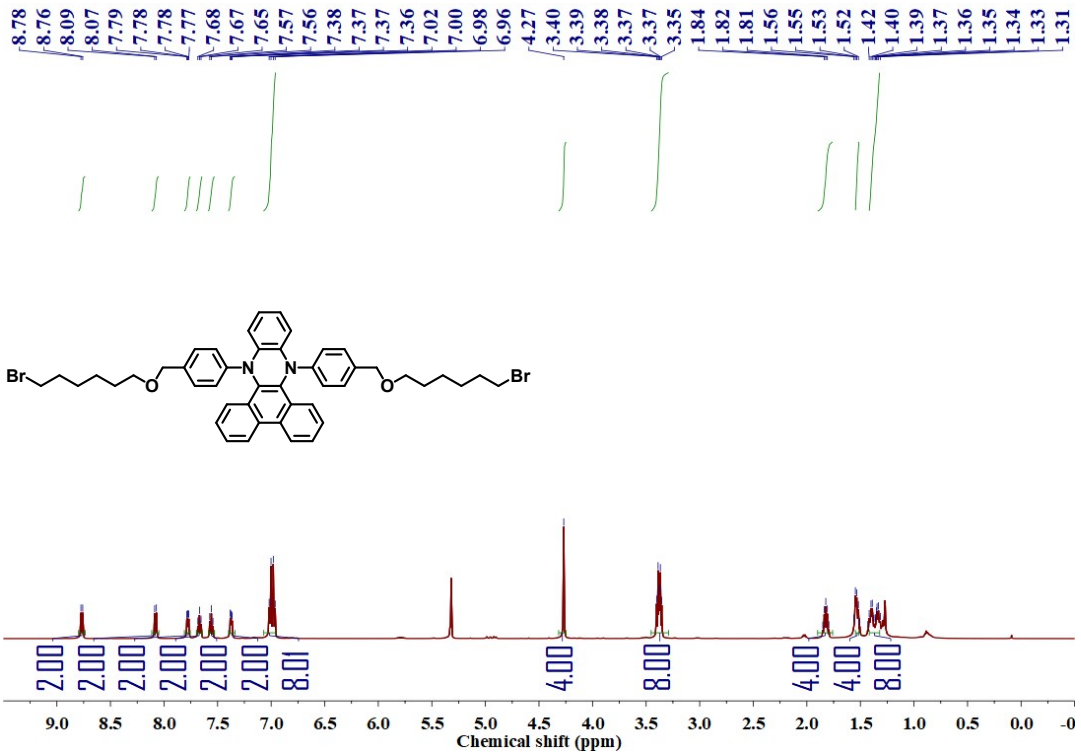

Figure S1. ^{1}H NMR spectrum (CD_2Cl_2, 298 K, 500 MHz) of compound **S2**.

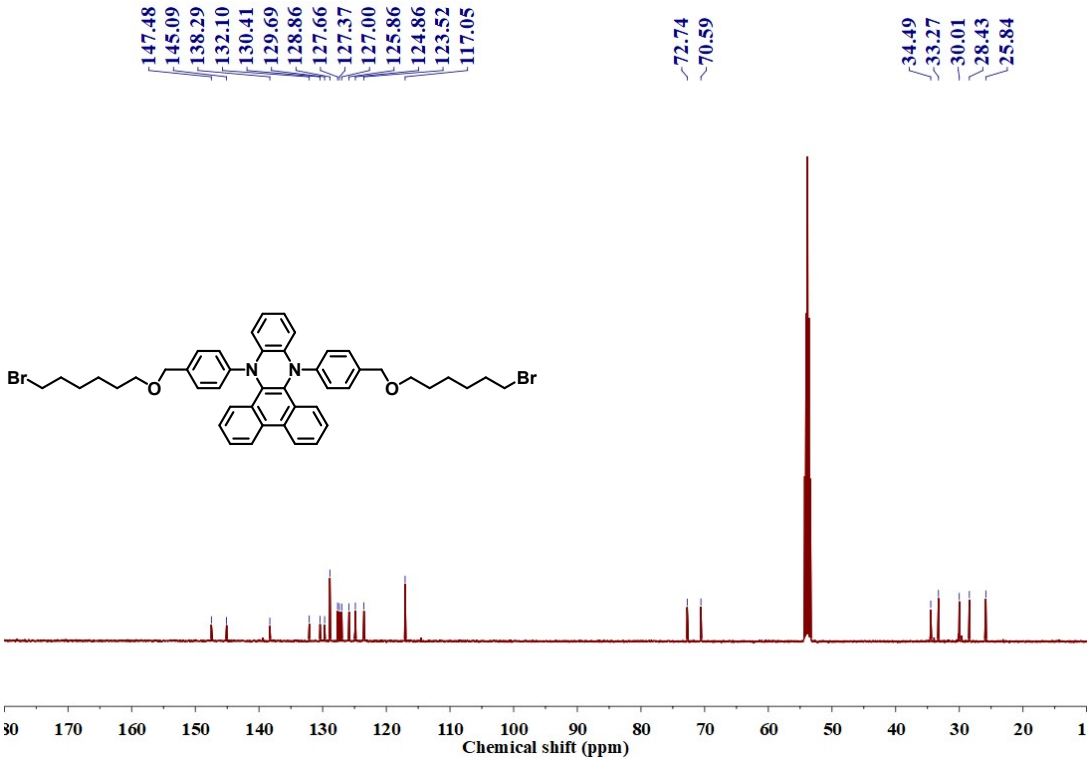

Figure S2. ^{13}C NMR spectrum (CD_2Cl_2, 298 K, 126 MHz) of compound **S2**.

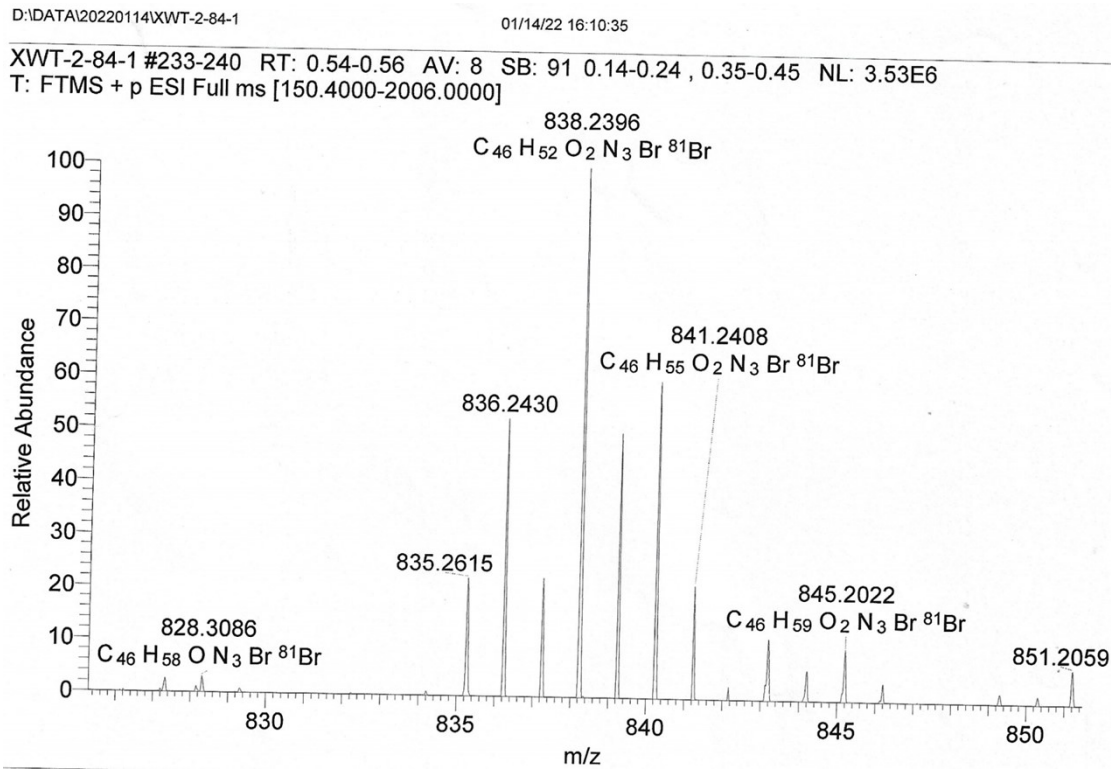

Figure S3. HRMS (ESI-TOF-MS) spectrum of compound **S2**.

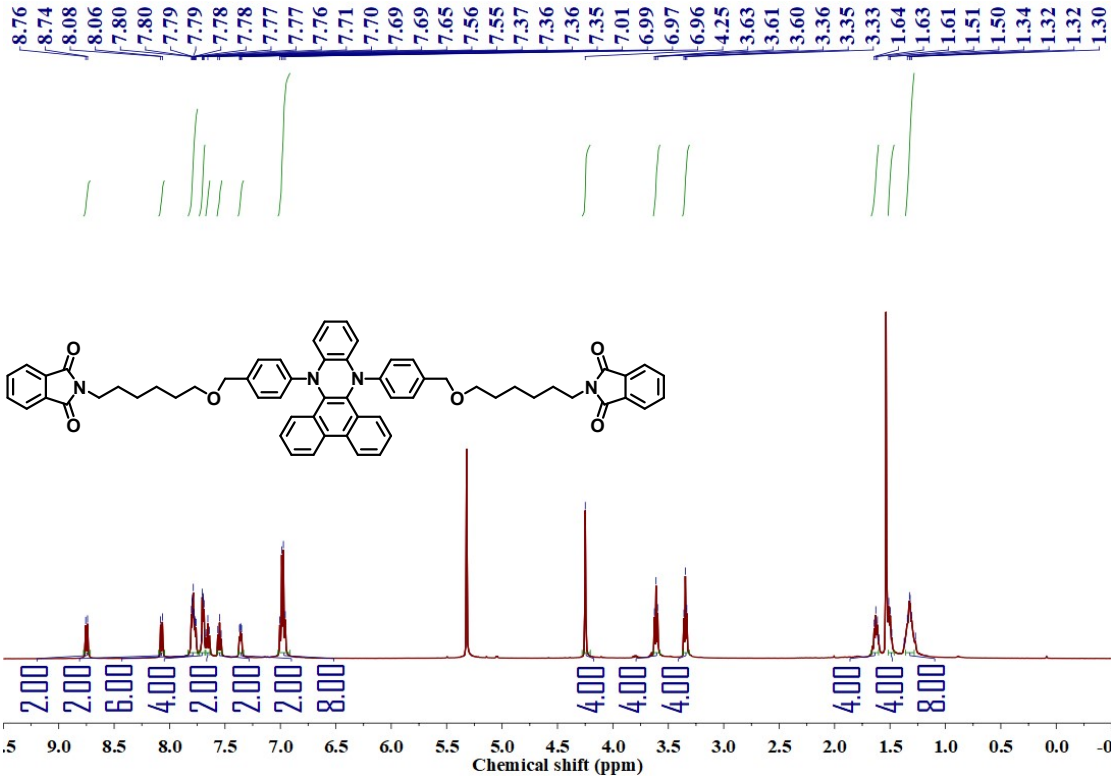

Figure S4. ^{1}H NMR spectrum (CD_2Cl_2, 298 K, 500 MHz) of compound **S3**.

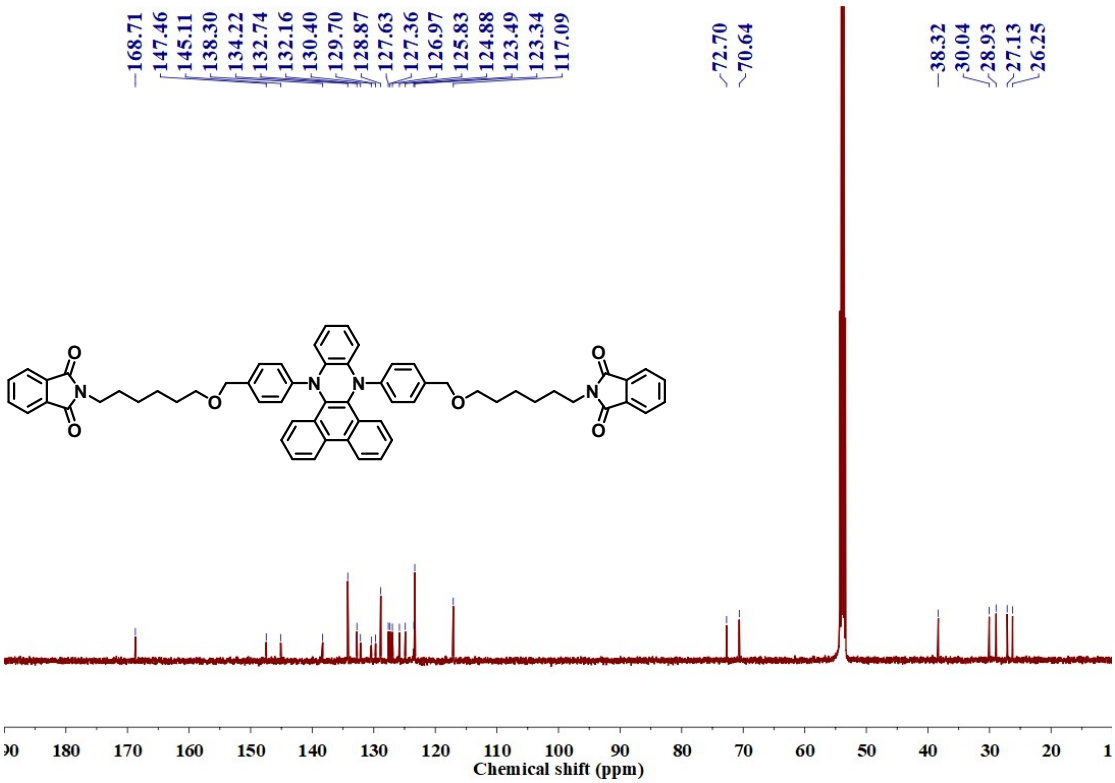

Figure S5. ^{13}C NMR spectrum (CD_2Cl_2, 298 K, 126 MHz) of compound **S3**.

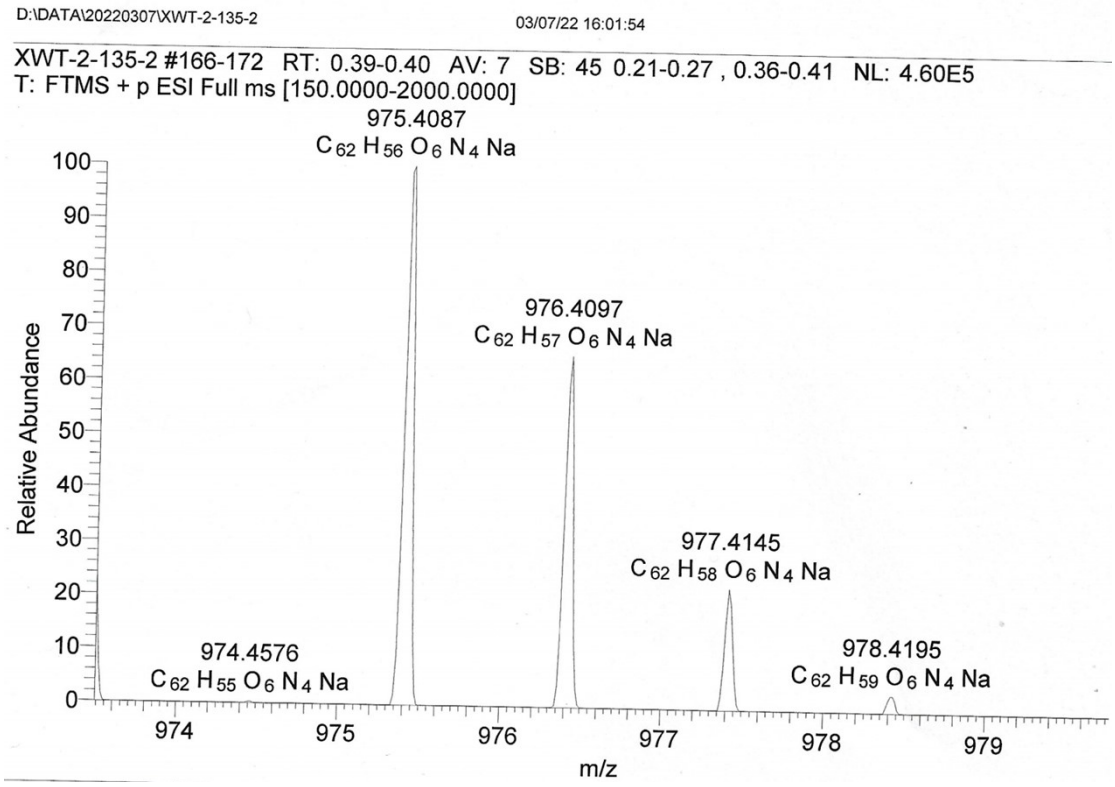

Figure S6. HRMS (ESI-TOF-MS) spectrum of compound **S3**.

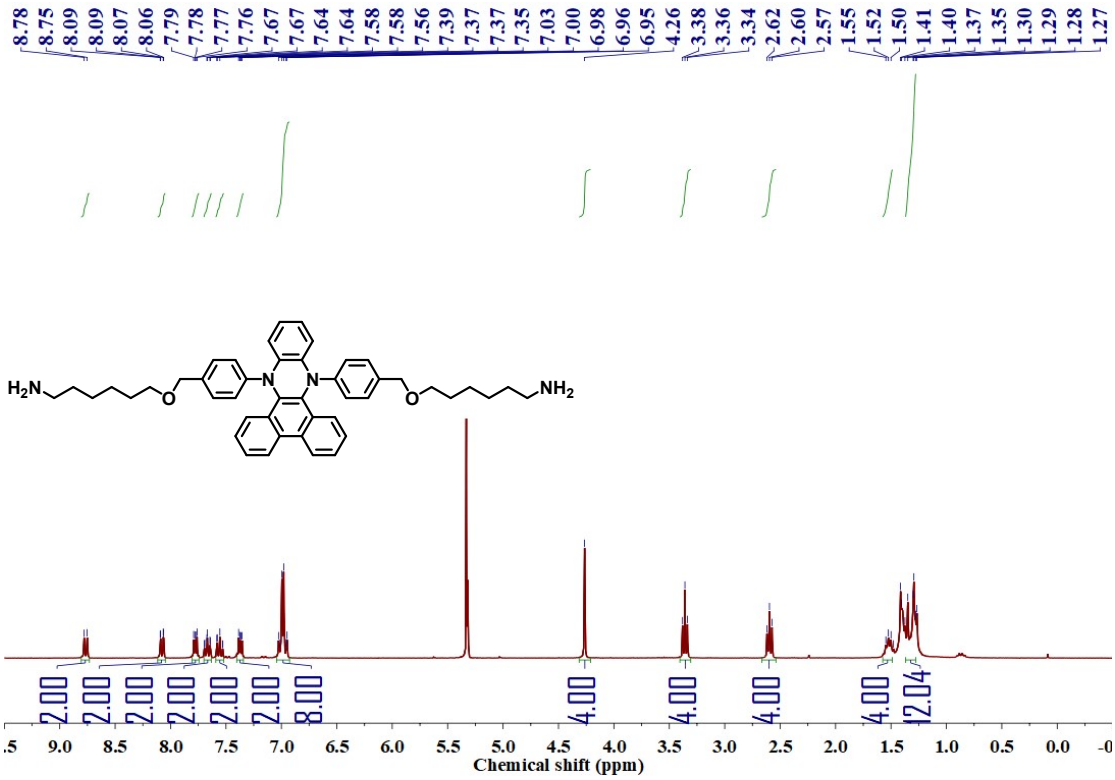

Figure S7. ^{1}H NMR spectrum (CD_2Cl_2, 298 K, 300 MHz) of compound **1**.

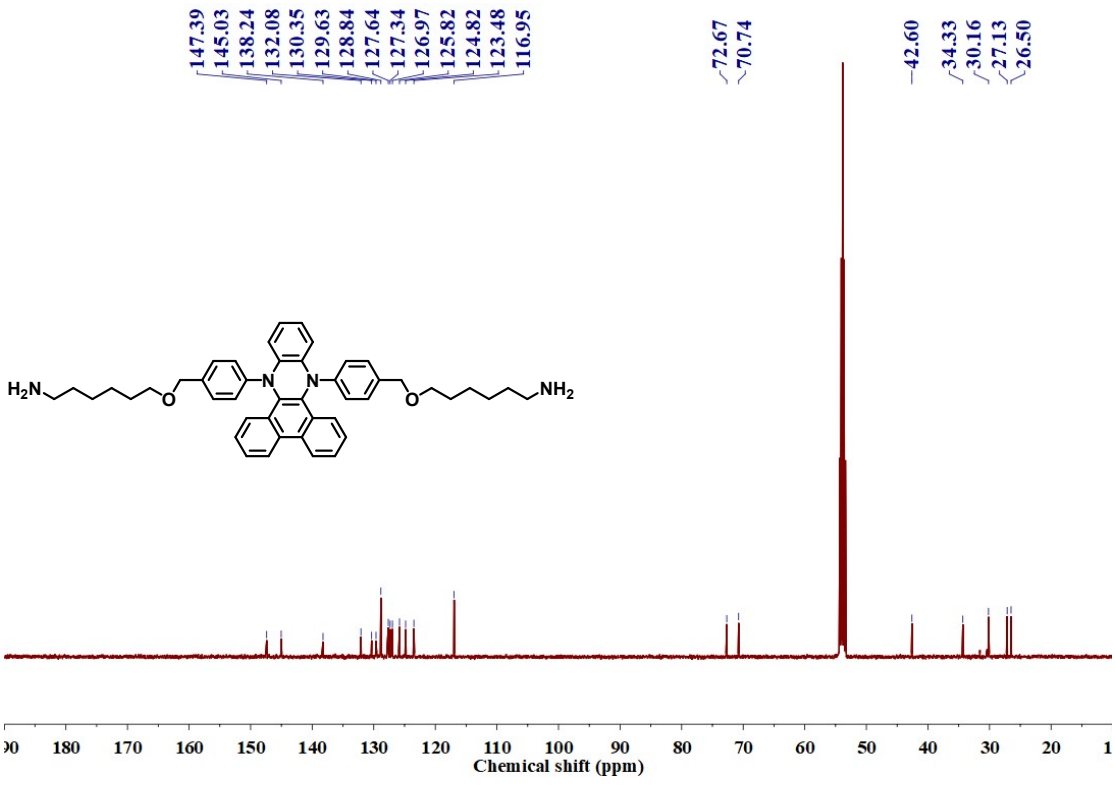

Figure S8. ^{13}C NMR spectrum (CD_2Cl_2, 298 K, 126 MHz) of compound **1**.

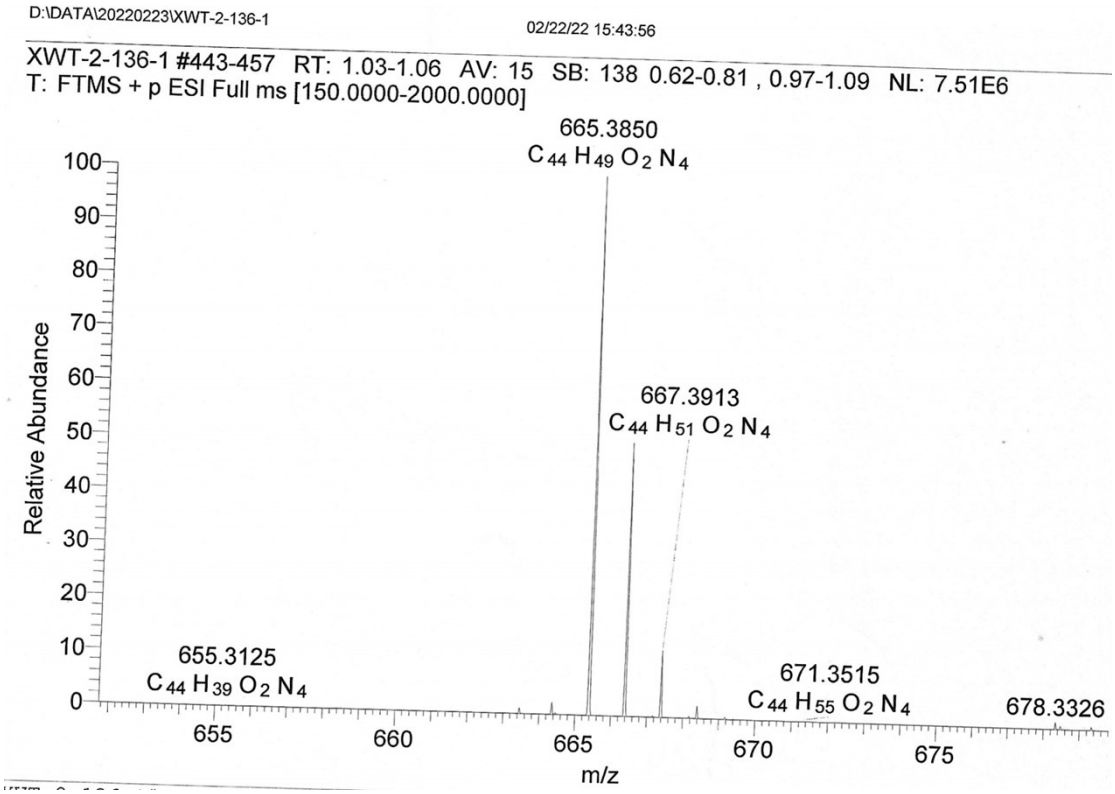

Figure S9. HRMS (ESI-TOF-MS) spectrum of compound **1**.

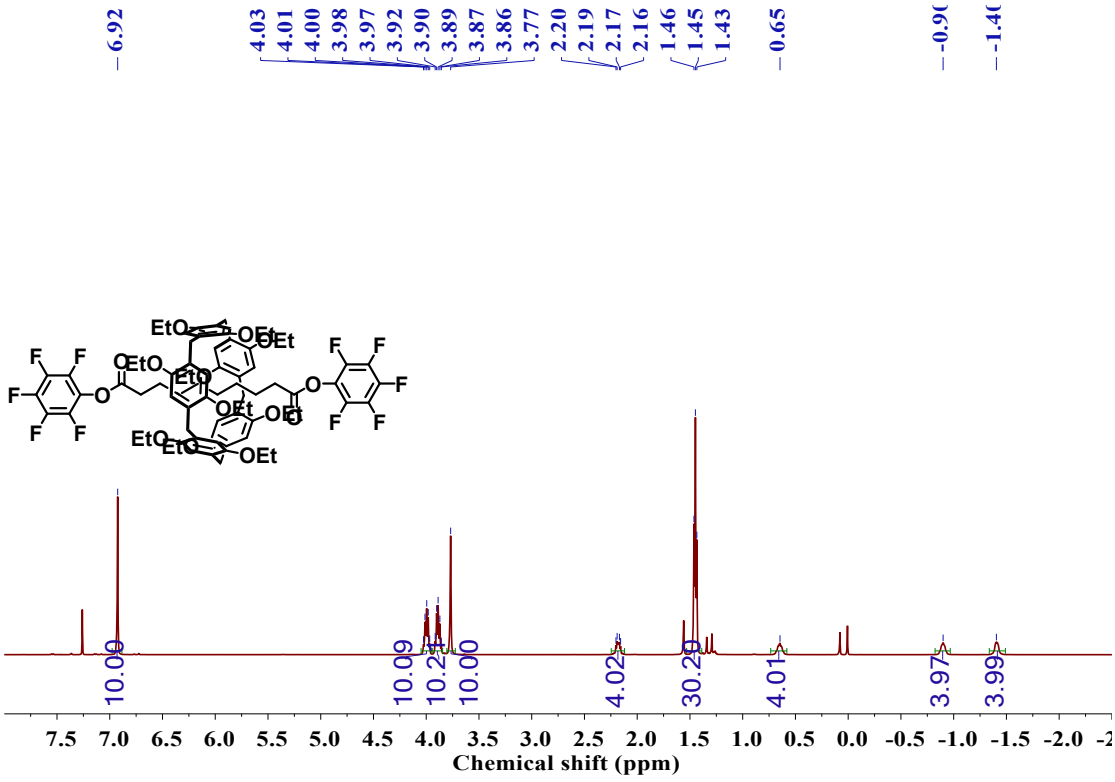

Figure S10. ^{1}H NMR spectrum ($CDCl_3$, 298 K, 500 MHz) of [2]rotaxane **2**.

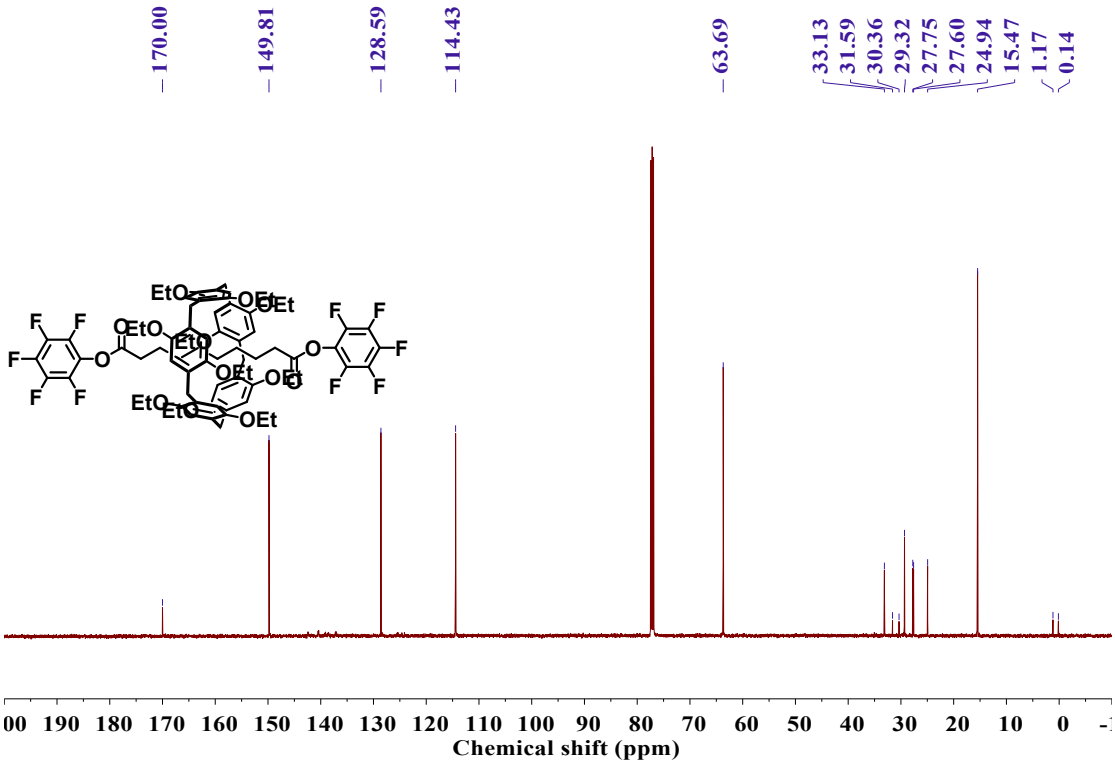

Figure S11. ^{13}C NMR spectrum ($CDCl_3$, 298 K, 126 MHz) of [2]rotaxane **2**.

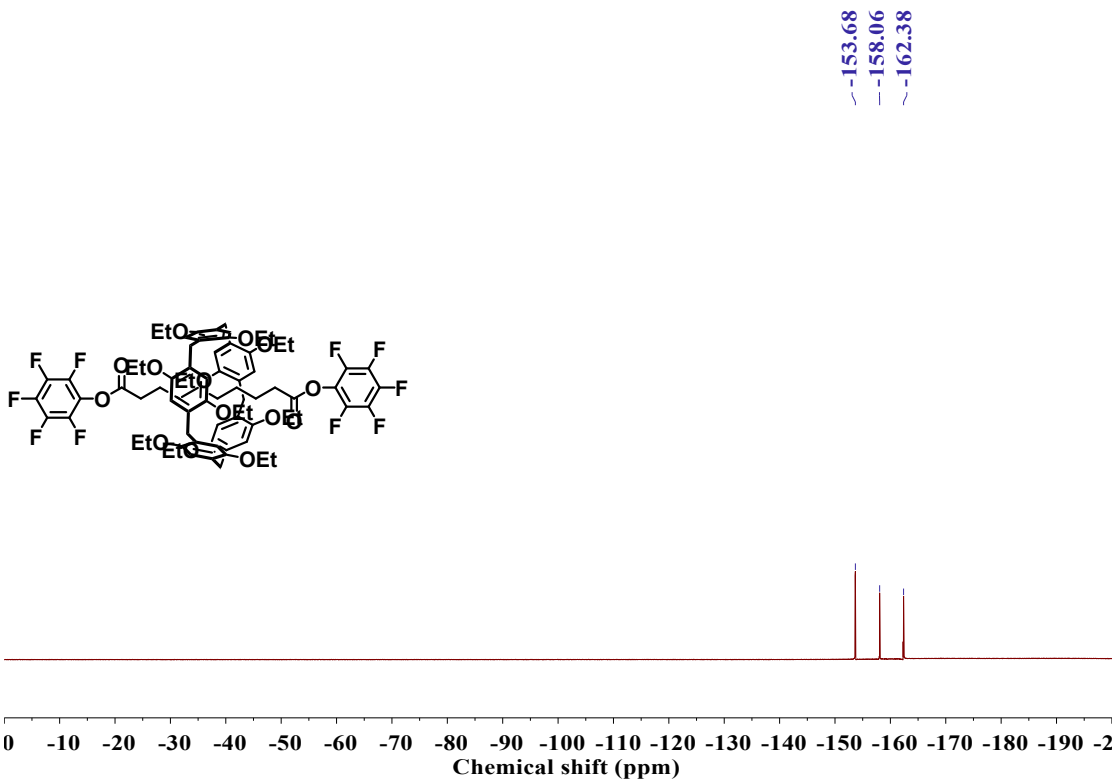

Figure S12. ^{19}F NMR spectrum ($CDCl_3$, 298 K, 376 MHz) of [2]rotaxane **2**.

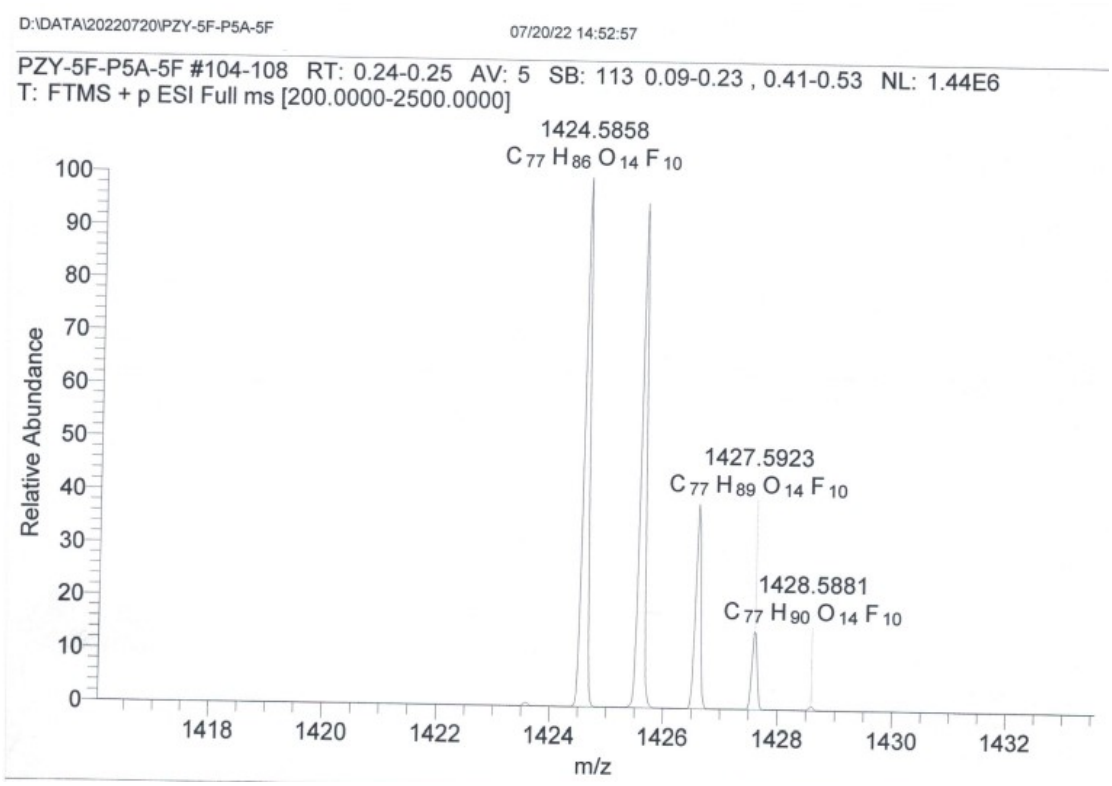

Figure S13. HRMS (ESI-TOF-MS) spectrum of [2]rotaxane **2**.

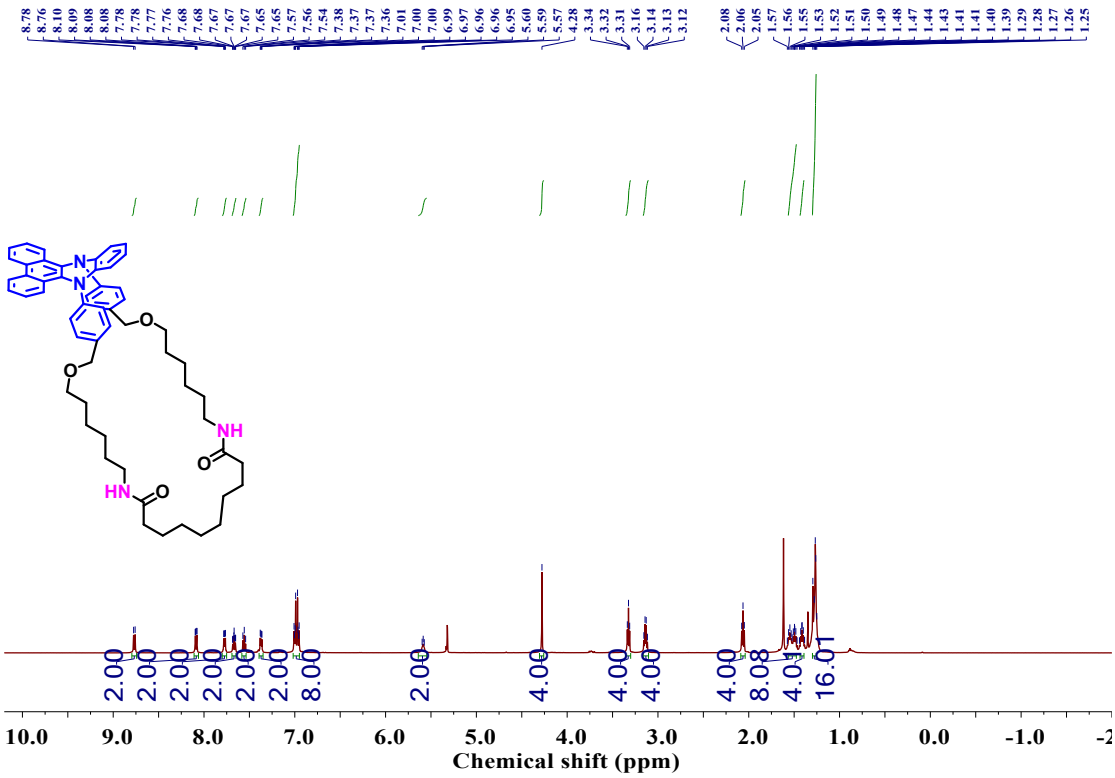

Figure S14. ^{1}H NMR spectrum (CD_2Cl_2, 298 K, 500 MHz) of macrocycle **DPAC-M**.

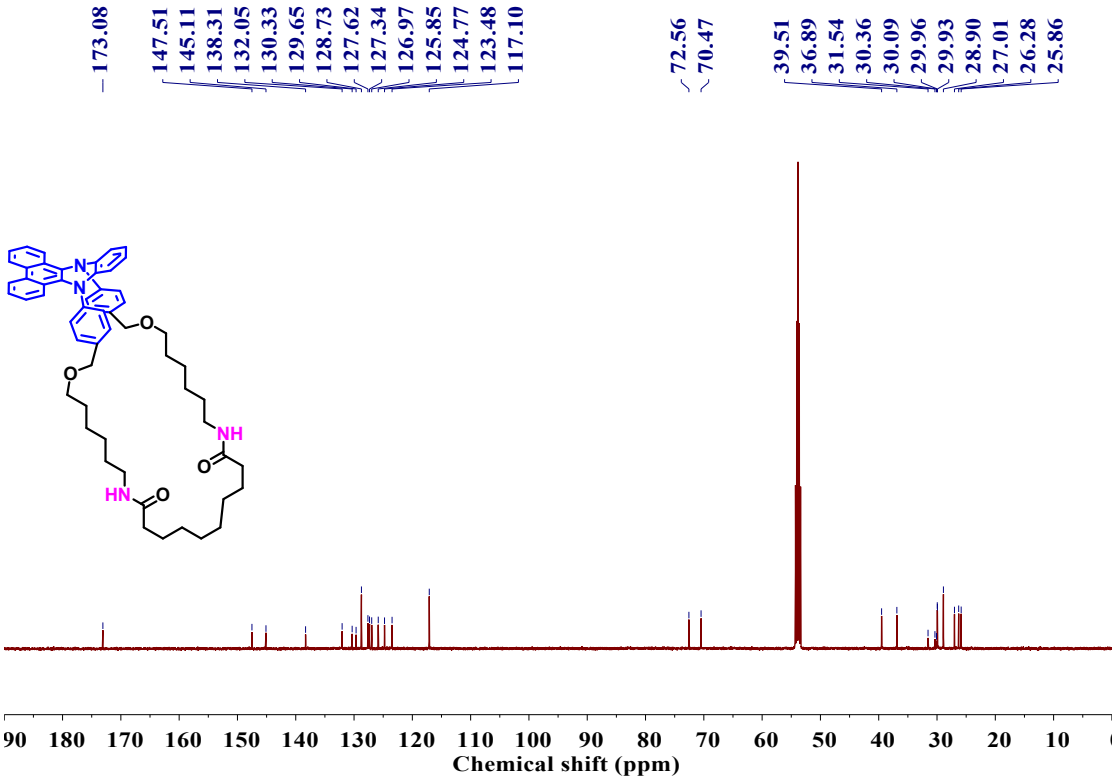

Figure S15. ^{13}C NMR spectrum (CD_2Cl_2, 298 K, 126 MHz) of macrocycle **DPAC-M**.

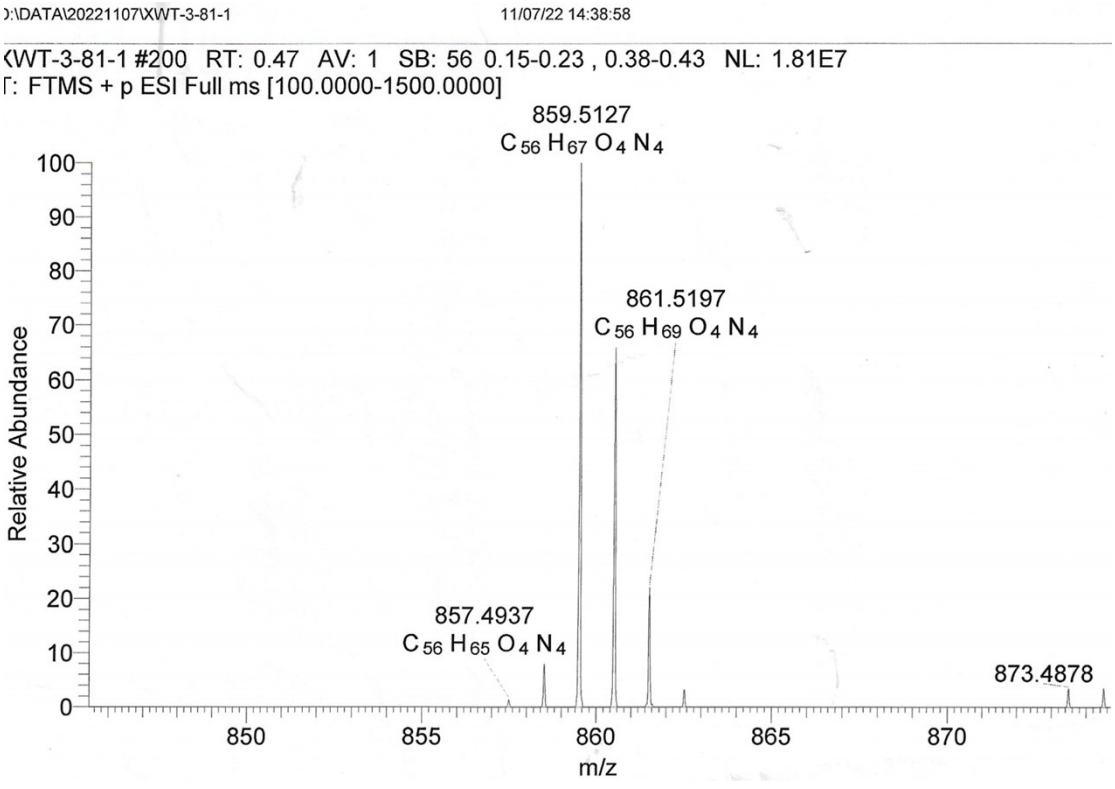

Figure S16. HRMS (ESI-TOF-MS) spectrum of macrocycle **DPAC-M**.

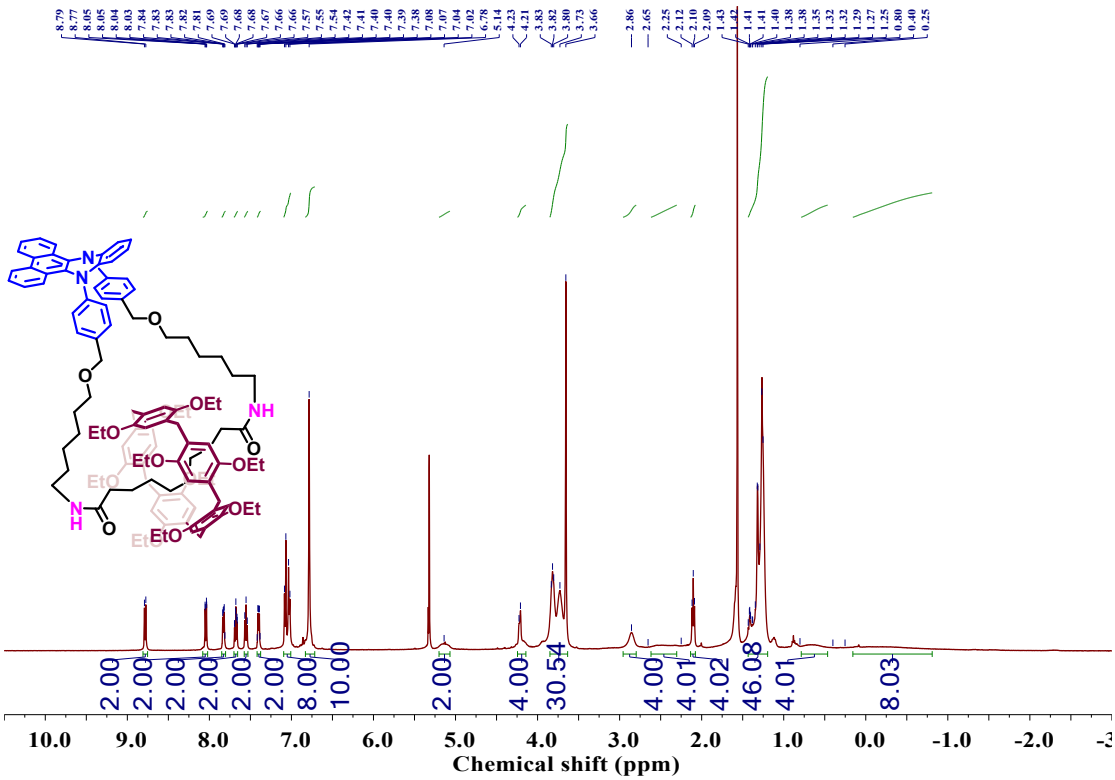

Figure S17. ^{1}H NMR spectrum (CD_2Cl_2, 298 K, 500 MHz) of [2]catenane **DPAC-C**.

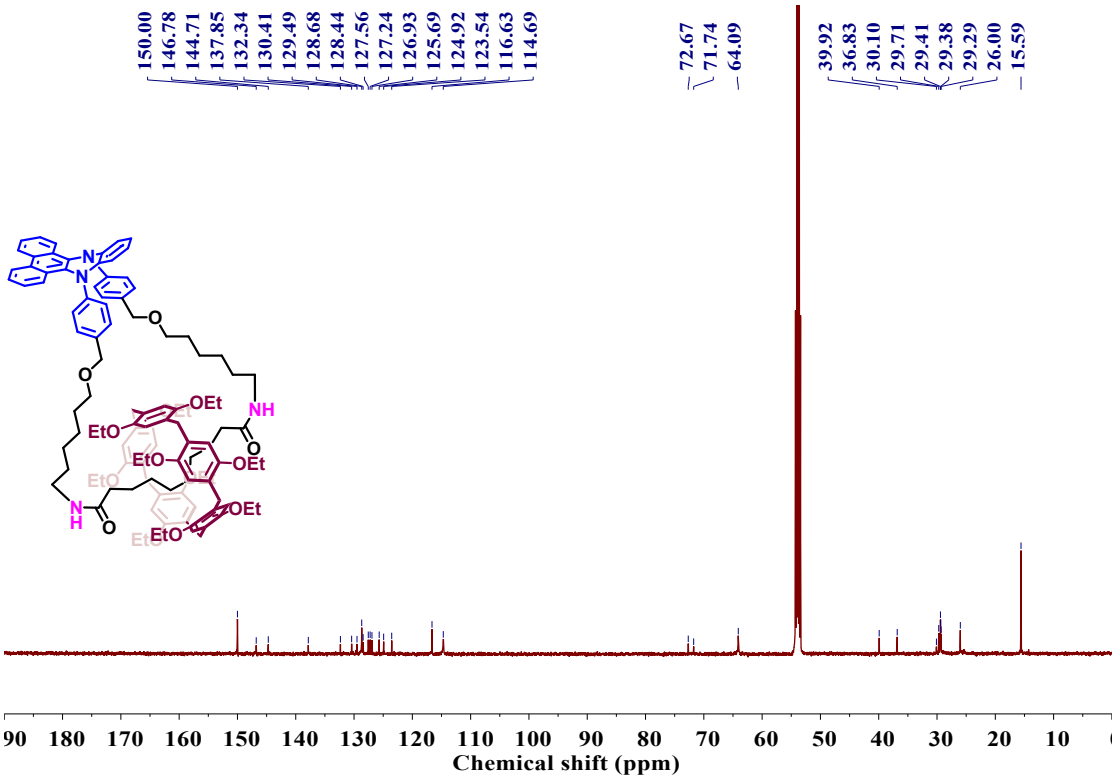

Figure S18. ^{13}C NMR spectrum (CD_2Cl_2, 298 K, 126 MHz) of [2]catenane **DPAC-C**.

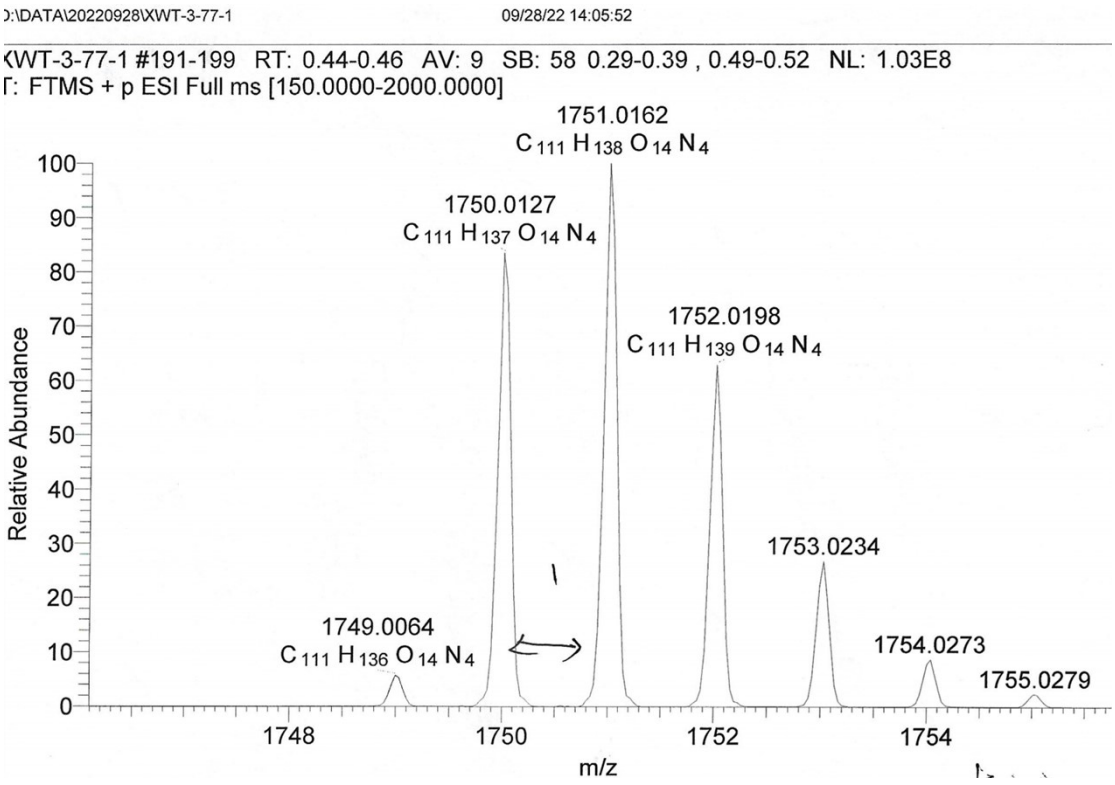

Figure S19. HRMS (ESI-TOF-MS) spectrum of [2]catenane **DPAC-C**.

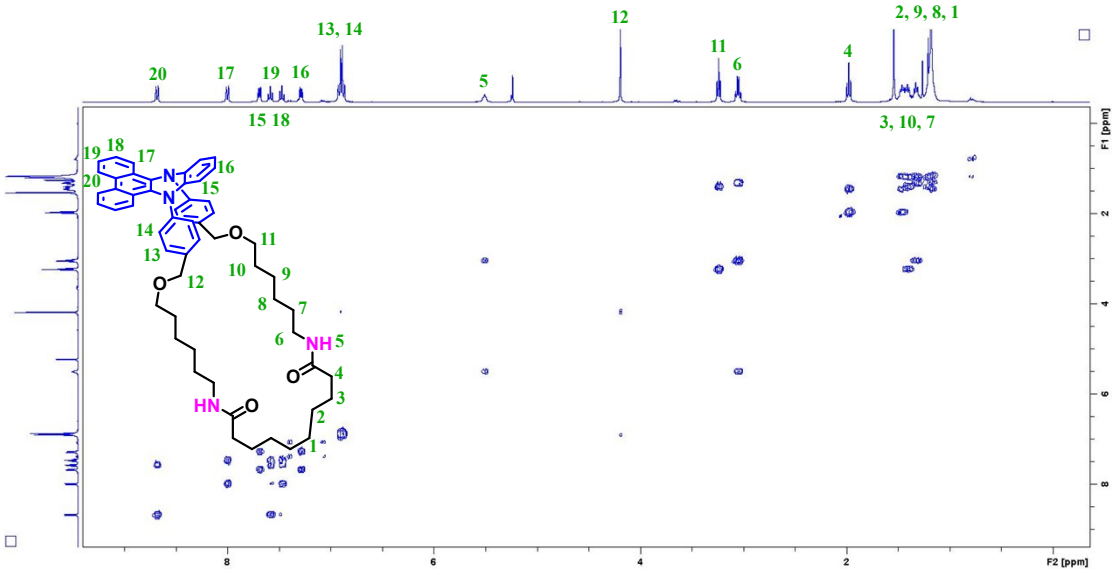

Figure S20. 2D ^{1}H-^{1}H COSY spectrum (CD_2Cl_2, 298 K, 500 MHz) of macrocycle **DPAC-M**.

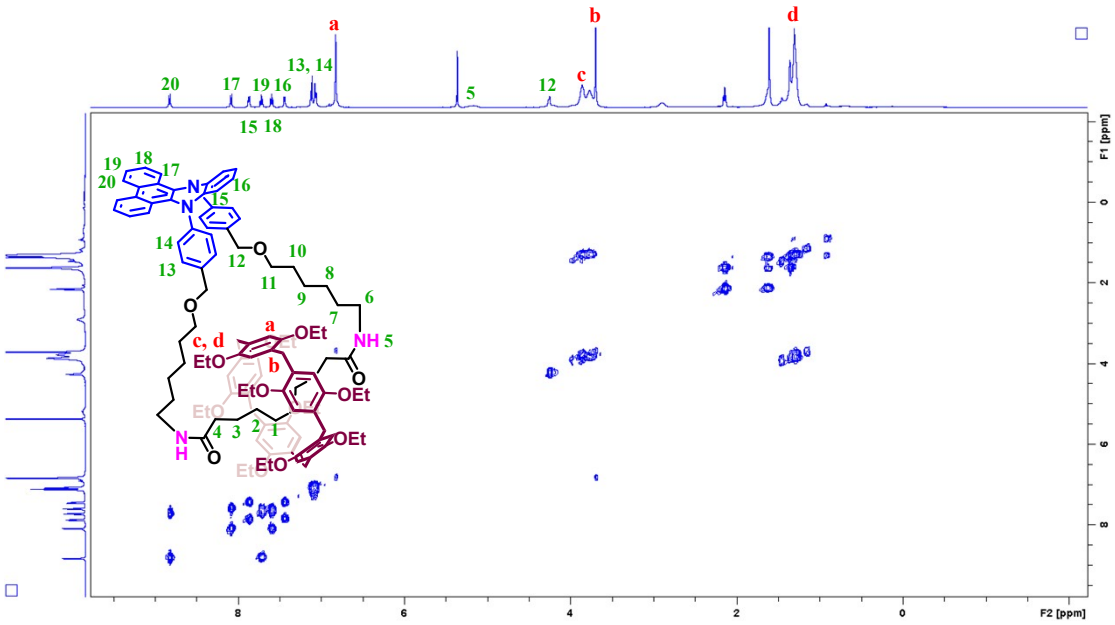

Figure S21. 2D ^{1}H-^{1}H COSY spectrum (CD_2Cl_2, 298 K, 500 MHz) of [2]catenane **DPAC-C**.

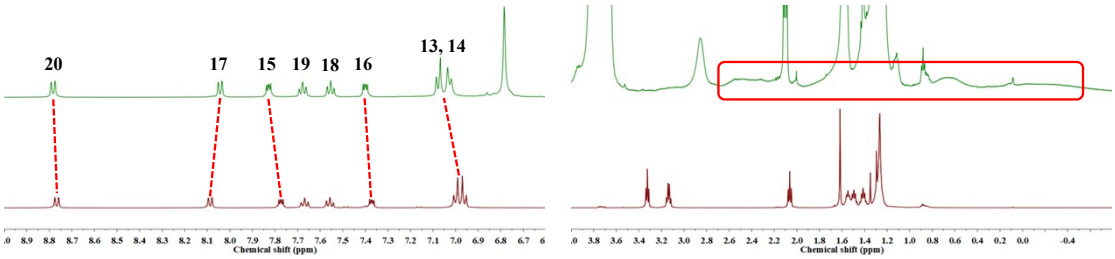

Figure S22. Partial ^{1}H NMR spectra (CD_2Cl_2, 298 K, 500 MHz) of macrocycle **DPAC-M** (*bottom*) and [2]catenane **DPAC-C** (*top*).

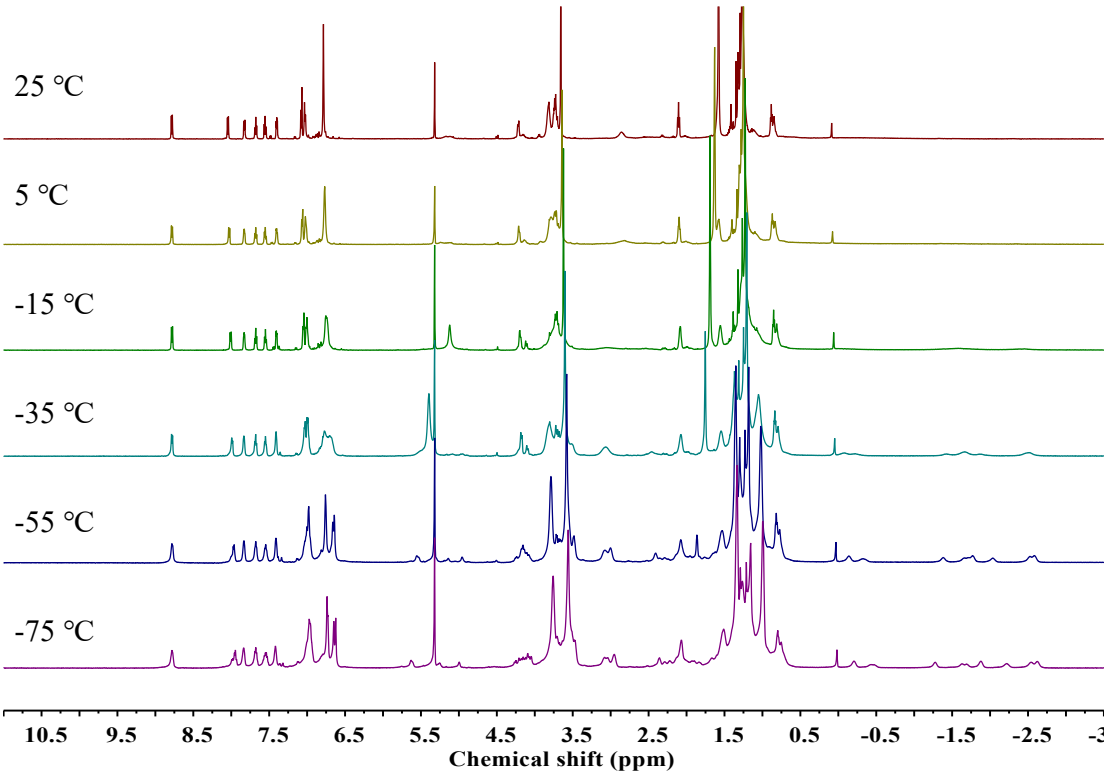

Figure S23. ^{1}H NMR spectra (CD_2Cl_2, 500 MHz) of [2]catenane **DPAC-C** at different temperatures.

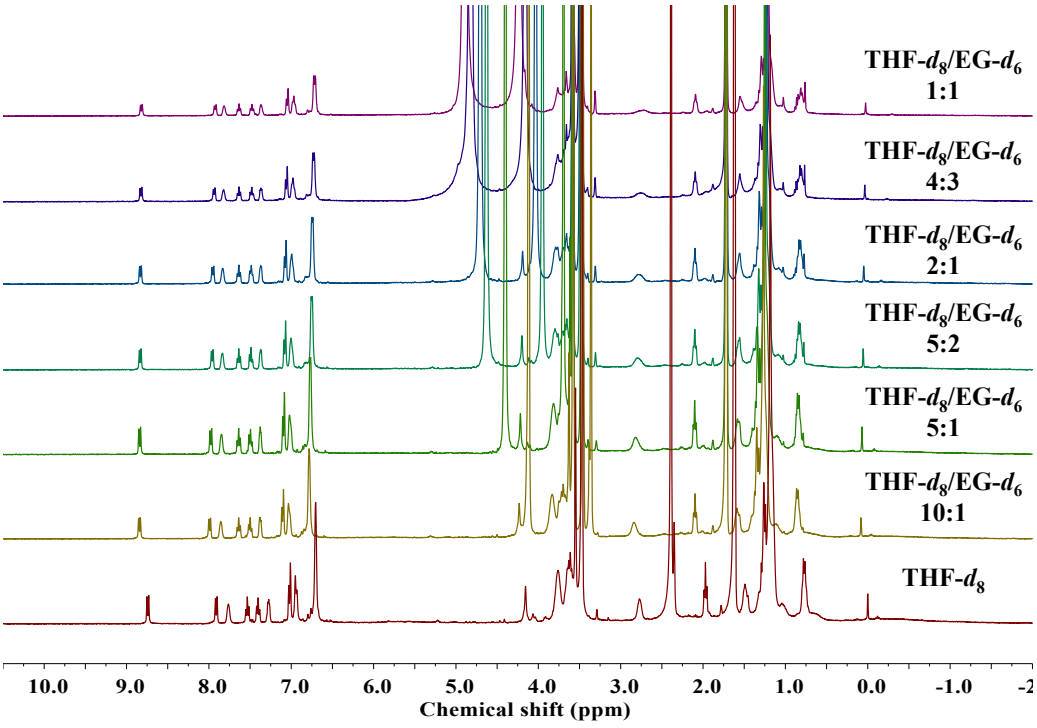

Figure S24. ^{1}H NMR spectra (298 K, 500 MHz) of [2]catenane **DPAC-C** in THF-d_8/EG-d_6 with

different EG-d_6 fractions.

Section C. Tunable VIE behaviors of macrocycle **DPAC-M** and [2]catenane **DPAC-C**.

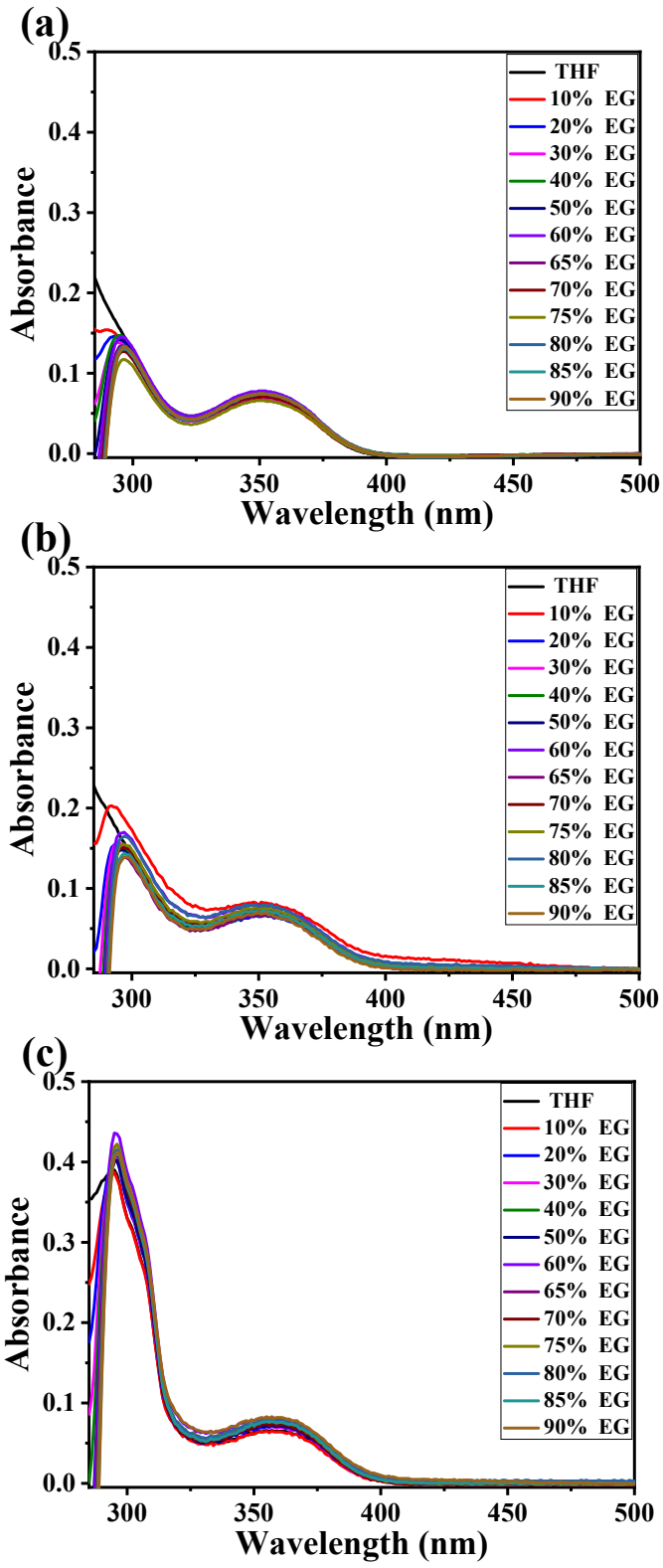

Figure S25. UV−vis absorption of macrocycle DPAC (a), **DPAC-M** (b), and [2]catenane **DPAC-C** (c) (0.01 mM) in THF/EG with different EG fractions.

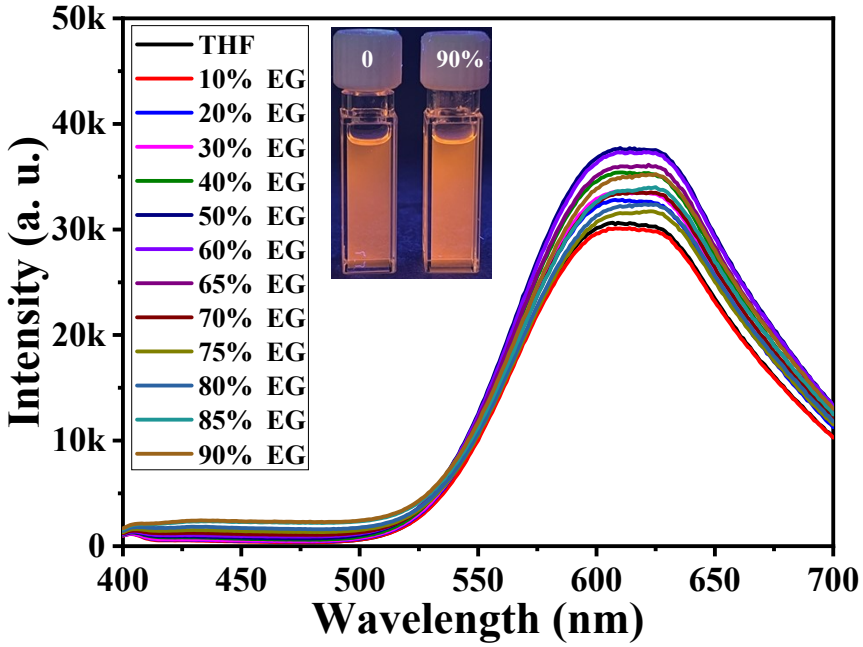

Figure S26. Fluorescence spectra of macrocycle DPAC (0.01 mM) in THF/EG with different EG fractions.

Table S1. Fluorescence quantum yields of macrocycle **DPAC-M** and [2]catenane **DPAC-C** (0.01 mM) in THF/EG with different EG fractions. Error: ± 0.1%.

EG (%)	0	10	20	30	40	50	60	65	70	75	80	85	90
DPAC-M	12.4	7.4	7.1	8.7	9.8	10.1	10.1	11.0	10.1	10.3	10.6	10.3	10.6
DPAC-C	18.6	17.8	17.1	20.3	22.4	24.0	25.3	24.9	26.3	27.1	29.0	28.3	32.0

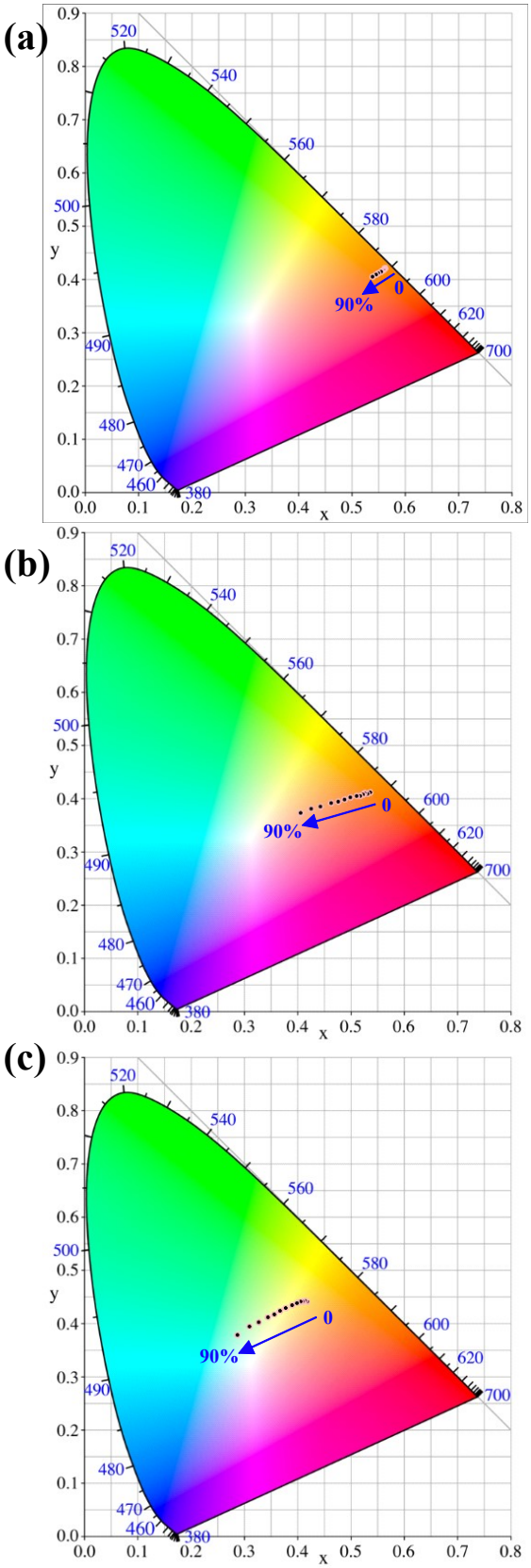

Figure S27. Corresponding 1931 CIE coordinate diagram of DPAC, macrocycle **DPAC-M**, and [2]catenane **DPAC-C** (0.01 mM) in THF/EG with different EG fractions.

Table S2. Corresponding 1931 CIE coordinates of DPAC, macrocycle **DPAC-M**, and [2]catenane **DPAC-C** (0.01 mM) in THF/EG with different EG fractions.

EG (%)	0	10	20	30	40	50	60	65	70	75	80	85	90
DPAC	(0.5618, 0.4213)	(0.563, 0.4219)	(0.5627, 0.4212)	(0.5626, 0.4208)	(0.5611, 0.4195)	(0.56, 0.4192)	(0.5583, 0.4174)	(0.5556, 0.416)	(0.5543, 0.4143)	(0.5492, 0.4115)	(0.5458, 0.4088)	(0.5389, 0.4051)	(0.539, 0.4053)
DPAC-M	(0.5364, 0.4122)	(0.5303, 0.4098)	(0.5251, 0.4113)	(0.5231, 0.4076)	(0.5167, 0.4057)	(0.5109, 0.4054)	(0.4993, 0.4022)	(0.4884, 0.3989)	(0.4755, 0.3951)	(0.4629, 0.3915)	(0.4429, 0.3853)	(0.4254, 0.381)	(0.4047, 0.3733)
DPAC-C	(0.4173, 0.4417)	(0.4139, 0.4426)	(0.4097, 0.442)	(0.4051, 0.4408)	(0.3987, 0.4384)	(0.3898, 0.4345)	(0.3778, 0.4287)	(0.367, 0.4236)	(0.3554, 0.4178)	(0.3442, 0.4124)	(0.3261, 0.4031)	(0.3096, 0.3951)	(0.2864, 0.3781)

Section D. Femtosecond transient absorption (TA) spectra of VIE-active macrocycle **DPAC-M** and [2]catenane **DPAC-C**.

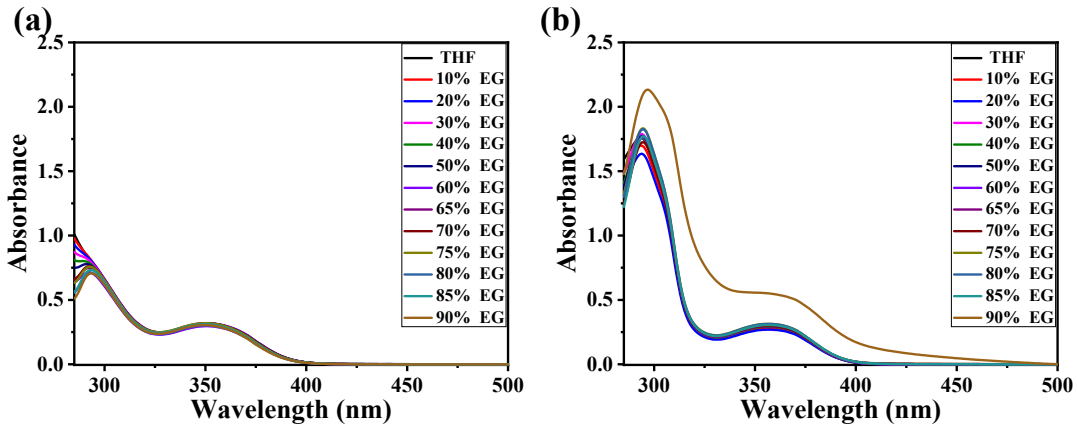

Figure S28. UV−vis absorption of macrocycle **DPAC-M** (a) and [2]catenane **DPAC-C** (b) (0.05 mM) in THF/EG with different EG fractions.

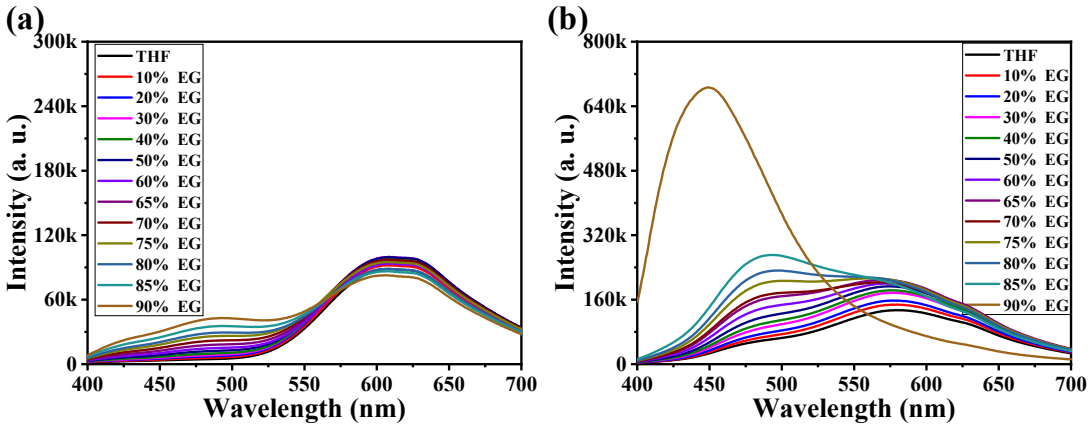

Figure S29. Fluorescence spectra of macrocycle **DPAC-M** (a) and [2]catenane **DPAC-C** (b) (0.05

mM) in THF/EG with different EG fractions.

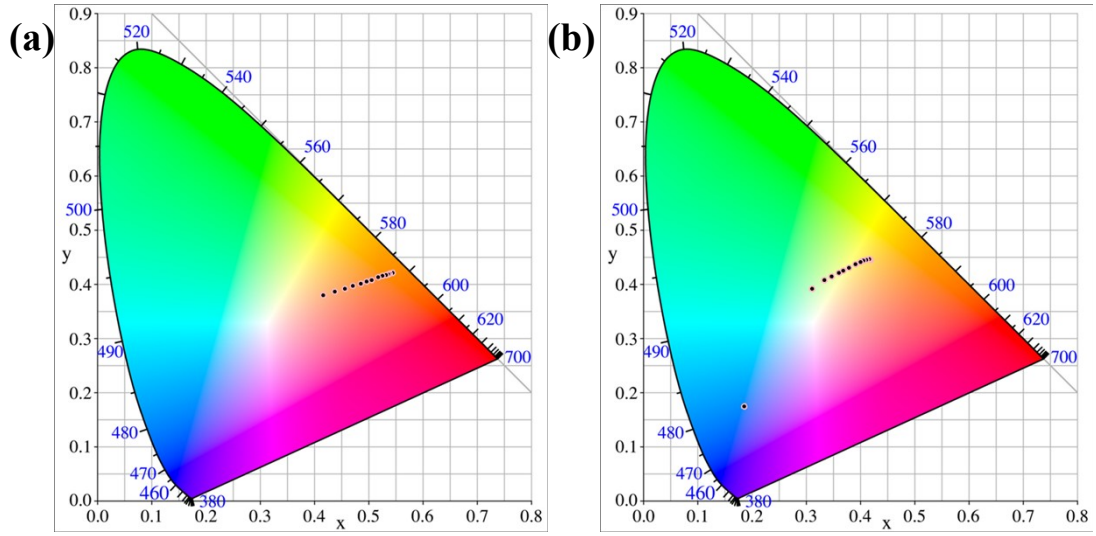

Figure S30. Corresponding 1931 CIE coordinate diagram of macrocycle **DPAC-M** and [2]catenane **DPAC-C** (0.05 mM) in THF/EG with different EG fractions.

Table S3. Corresponding 1931 CIE coordinates of macrocycle **DPAC-M** and [2]catenane **DPAC-C** (0.05 mM) in THF/EG with different EG fractions.

EG (%)	0	10	20	30	40	50	60	65	70	75	80	85	90
DPAC-M	(0.5436, 0.4211)	(0.5389, 0.4202)	(0.5355, 0.4187)	(0.5315, 0.4177)	(0.5259, 0.4156)	(0.5178, 0.4128)	(0.5055, 0.4086)	(0.4962, 0.4055)	(0.4851, 0.4018)	(0.4708, 0.3972)	(0.4563, 0.3924)	(0.4377, 0.3864)	(0.4157, 0.3794)
DPAC-C	(0.4189, 0.4455)	(0.4154, 0.4467)	(0.4108, 0.4454)	(0.4059, 0.4437)	(0.3995, 0.441)	(0.3912, 0.4372)	(0.3783, 0.4308)	(0.3686, 0.4259)	(0.3595, 0.4213)	(0.3468, 0.4147)	(0.3328, 0.4074)	(0.3109, 0.3926)	(0.1847, 0.1751)

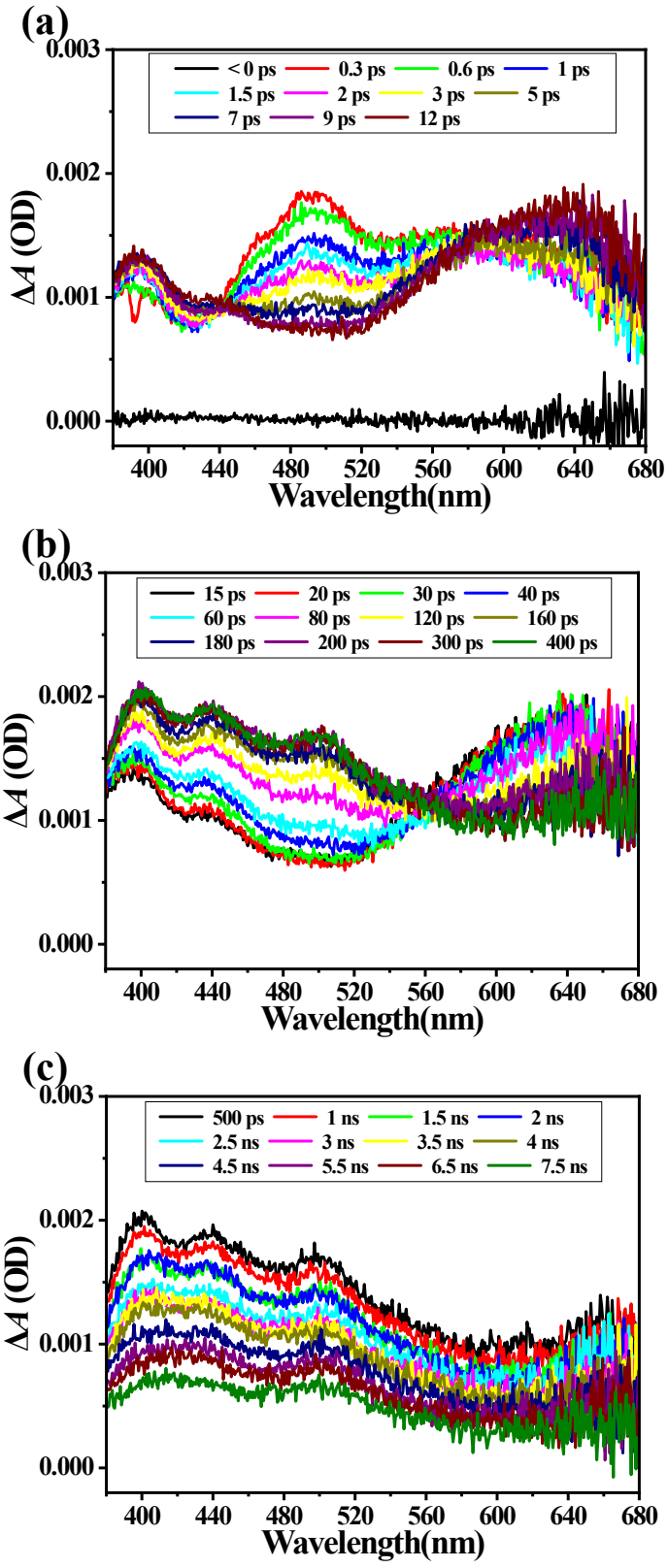

Figure S31. Femtosecond transient absorption spectra of macrocycle **DPAC-M** in THF with a photoexcitation of 360 nm at different time points.

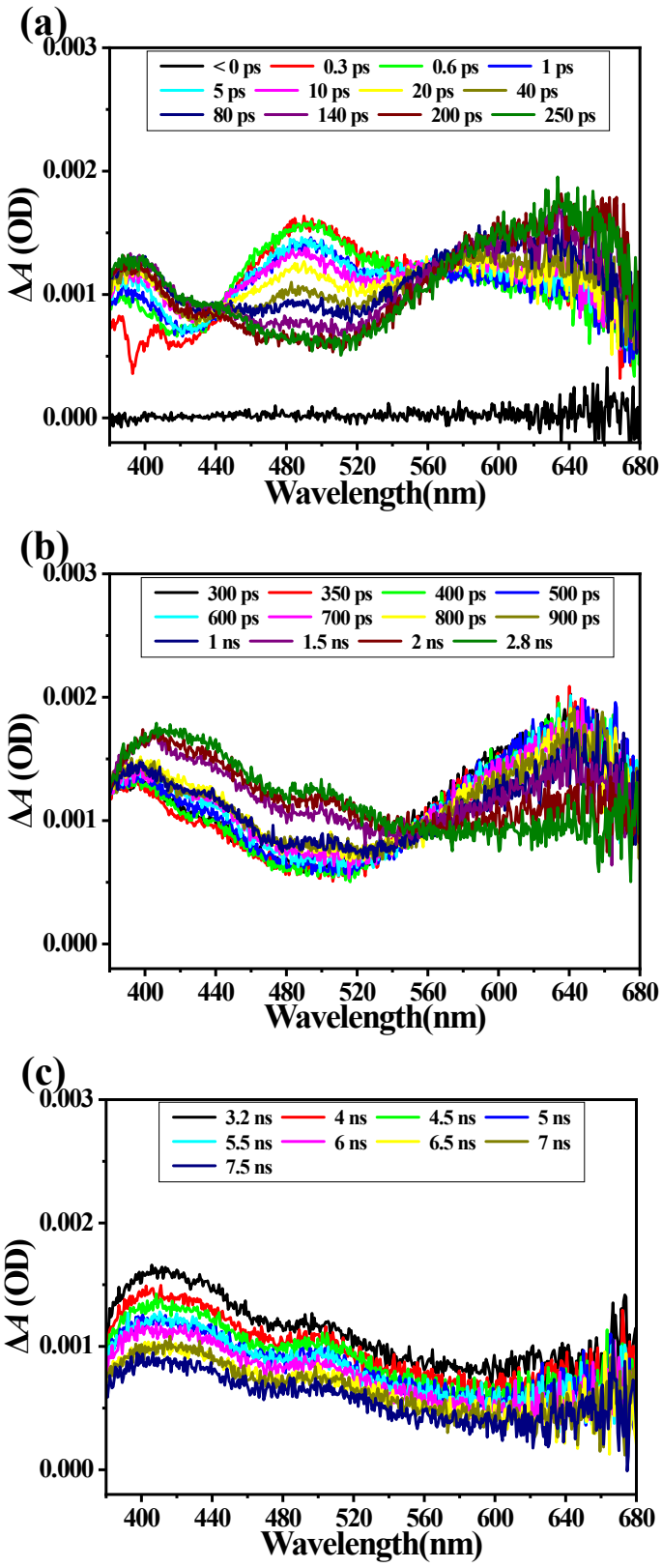

Figure S32. Femtosecond transient absorption spectra of macrocycle **DPAC-M** in THF/EG (v/v = 10/90) with a photoexcitation of 360 nm at different time points.

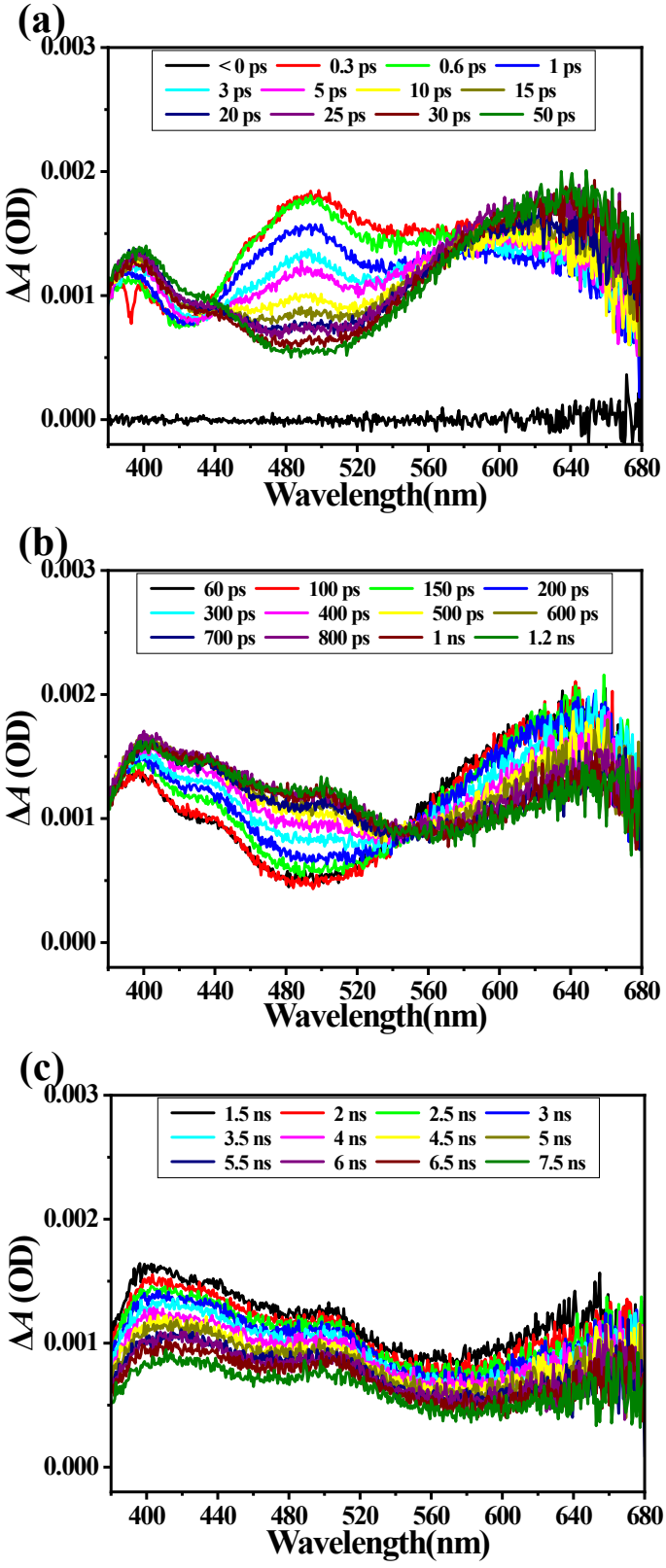

Figure S33. Femtosecond transient absorption spectra of [2]catenane **DPAC-C** in THF with a photoexcitation of 360 nm at different time points.

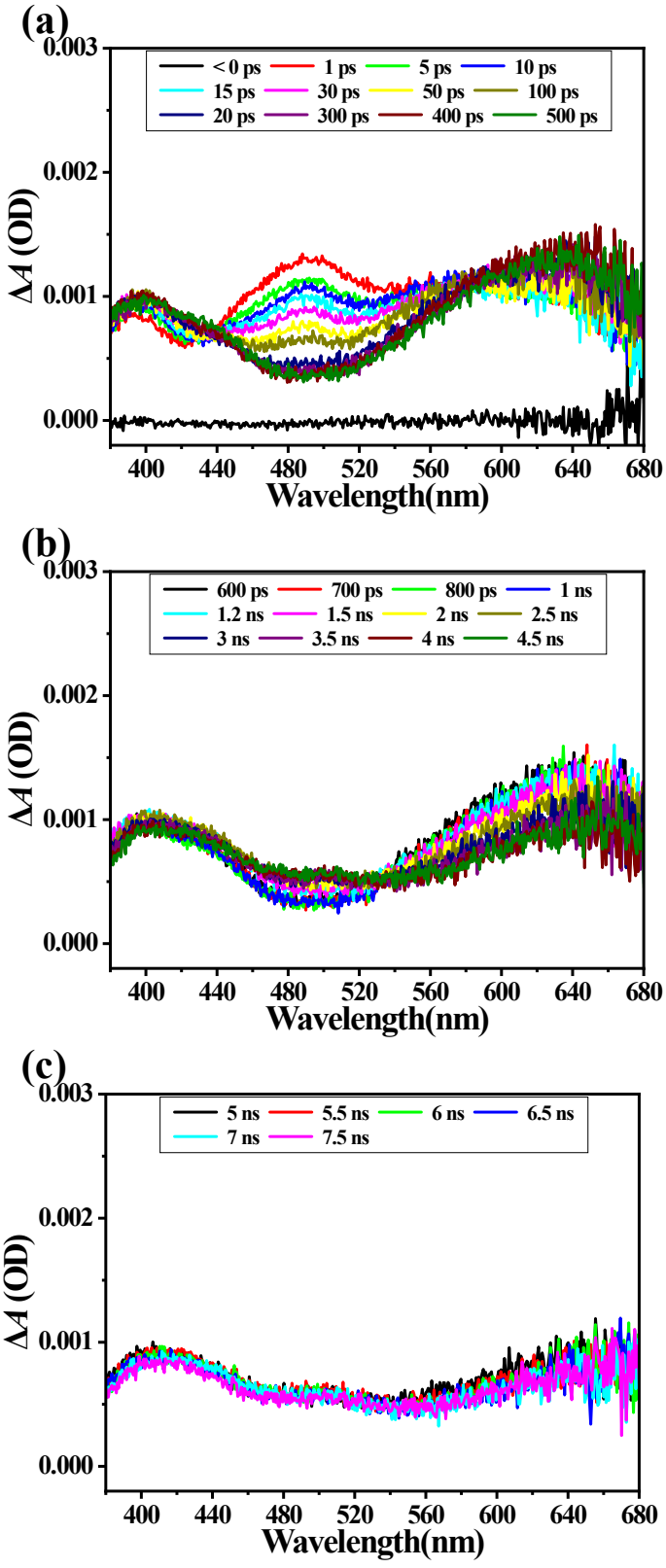

Figure S34. Femtosecond transient absorption spectra of [2]catenane **DPAC-C** in THF/EG (v/v = 15/85) with a photoexcitation of 360 nm at different time points.

Notably, in this study, on the basis of previous reports (*e.g.* Tian, Zhang, Chen *et al. Angew. Chem. Int. Ed.* 2023, 62, e202305572.), the species of the steady state fluorescence spectra were allocated using their relationship with stimulated emission (SE) in TA. However, it is undeniable that species observed in TA might be dark or have very low luminescence oscillator intensity.

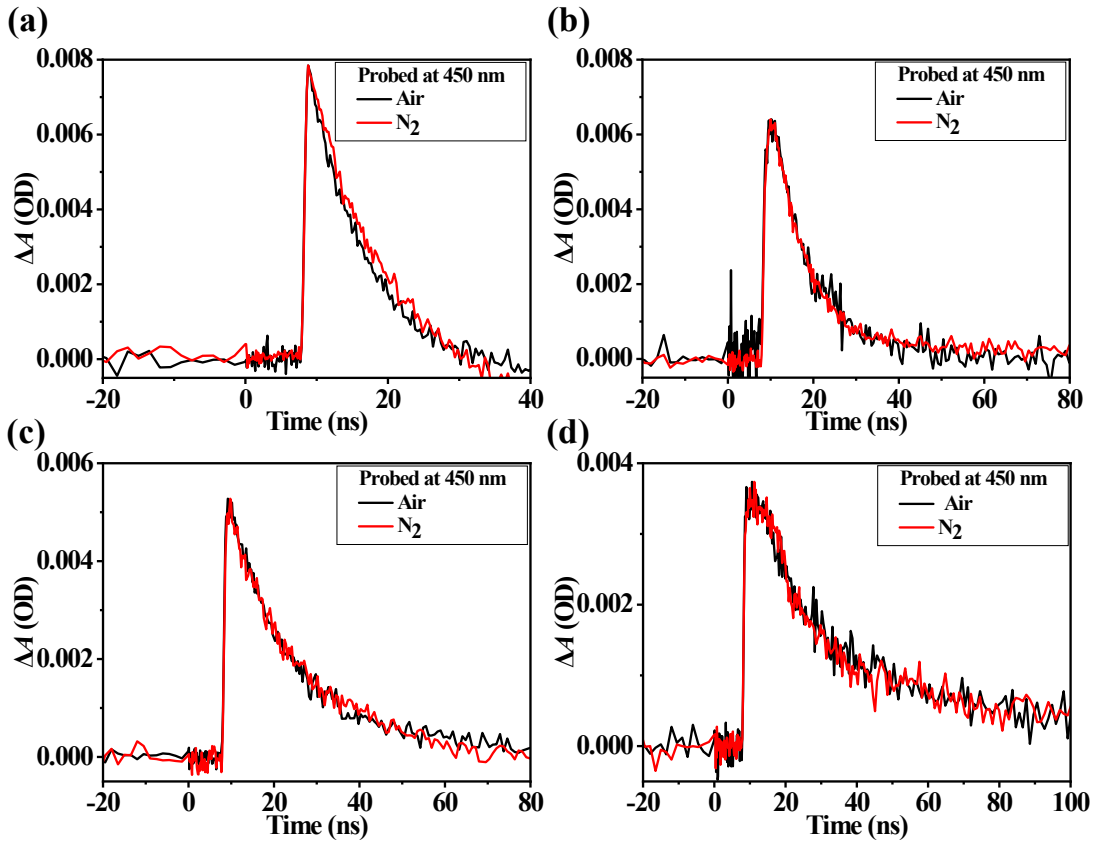

Figure S35. The kinetics curves at 450 nm probed wavelengths of **DPAC-M** in air-atmosphere and nitrogen-bubbled THF (a) and THF/EG (v/v = 10/90) (b). The kinetics curves at 450 nm probed wavelengths of **DPAC-C** in air-atmosphere and nitrogen-bubbled THF (c) and THF/EG (v/v = 15/85) (d).

Section E. HPLC traces of [2]catenane **DPAC-C**.

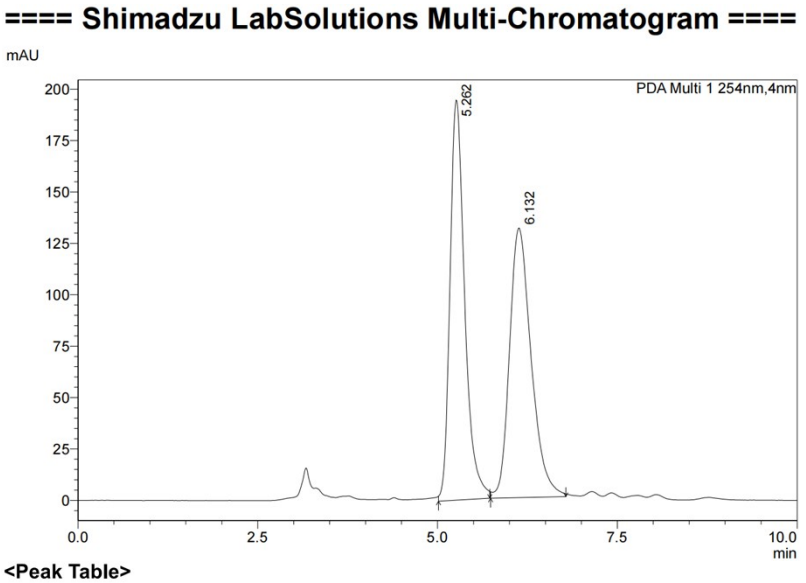

<Peak Table>
PDA Ch1 254nm

Peak#	Ret. Time	Area	Height	Conc.	Unit	Mark	Name
1	5.262	2763820	194619	0.000		M	
2	6.132	2750690	131129	0.000		M	
Total		5514510	325748				

Figure S36. Chiral HPLC analysis [column, CHIRALPAK IC® column (250 mm L × 4.6 mm I. D.); eluent, ethyl acetate: n-hexane (30:70); flow rate, 1.0 mL/ min; detection, 254 nm] of the *rac*-[2]catenane **DPAC-C**.

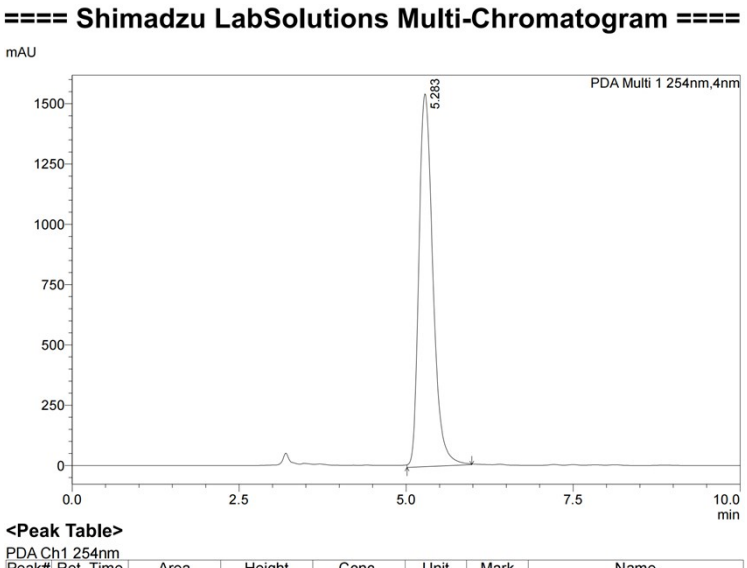

<Peak Table>
PDA Ch1 254nm

Peak#	Ret. Time	Area	Height	Conc.	Unit	Mark	Name
1	5.283	22577633	1545308	0.000		M	
Total		22577633	1545308				

Figure S37. Chiral HPLC analysis [column, CHIRALPAK IC® column (250 mm L × 4.6 mm I. D.); eluent, ethyl acetate: n-hexane (30:70); flow rate, 1.0 mL/ min; detection, 254 nm] of the *pS*-[2]catenane **DPAC-C**.

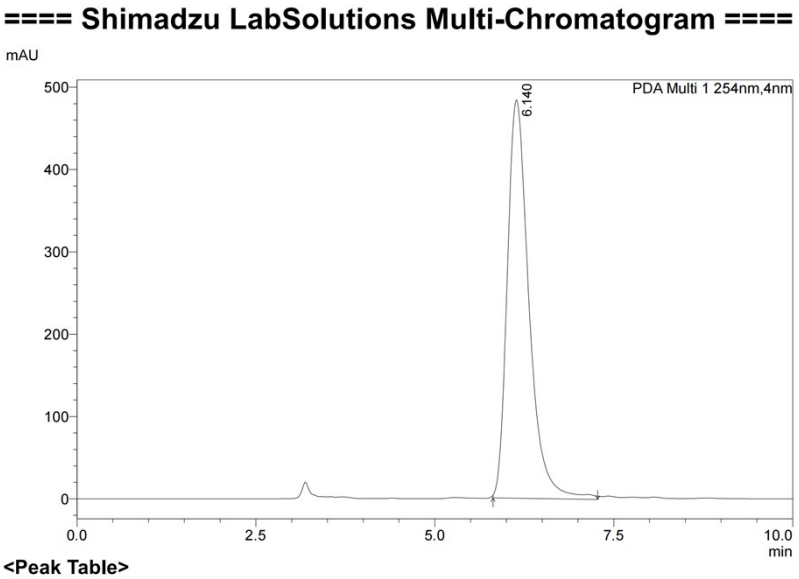

<Peak Table>
PDA Ch1 254nm

Peak#	Ret. Time	Area	Height	Conc.	Unit	Mark	Name
1	6.140	10202229	483836	0.000		M	
Total		10202229	483836				

Figure S38. Chiral HPLC analysis [column, CHIRALPAK IC® column (250 mm L × 4.6 mm I. D.); eluent, ethyl acetate: n-hexane (30:70); flow rate, 1.0 mL/ min; detection, 254 nm] of the *pR*-[2]catenane **DPAC-C**.

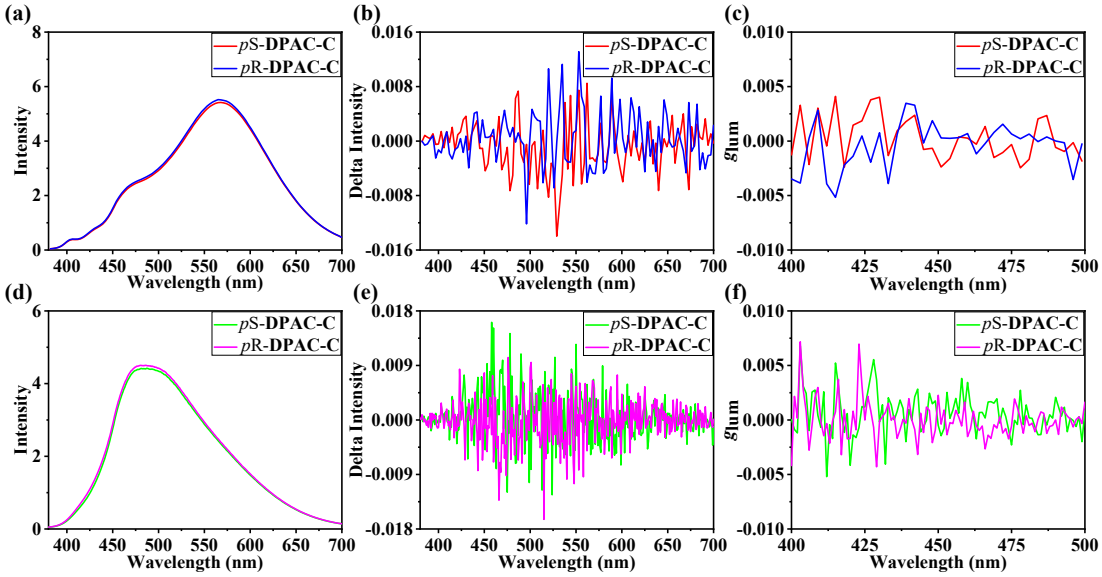

Figure S39. Fluorescence intensity (a, d), delta intensity (b, e), and g_{lum} (c, f) of chiral [2]catenanes *pS*/*pR*-**DPAC-C** in THF and in THF/EG (v/v = 10/90).

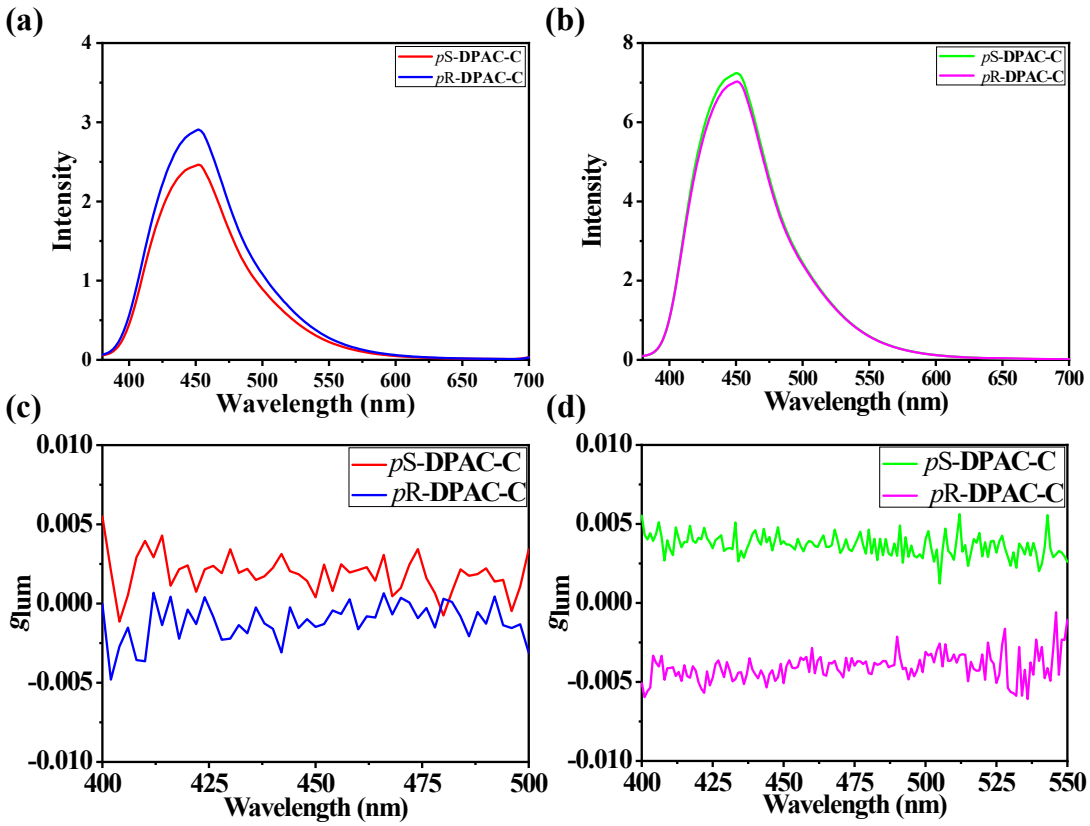

Figure S40. Fluorescence intensity (a, b) and g_{lum} of chiral [2]catenanes *pS*/*pR*-**DPAC-C** in casted films and in KBr pellets (c, 2.46 × 10^{-3}/-2.68 × 10^{-3}; d, 4.79 × 10^{-3}/-5.08 × 10^{-3}).

Section F. References.

[1] W. Chen, C. Guo, Q. He, X. Chi, V. M. Lynch, Z. Zhang, J. Su, H. Tian, J. L. Sessler, *J. Am. Chem. Soc.* **2019**, *141*, 14798-14806

[2] T. Ogoshi, N. Ueshima, F. Sakakibara, T.-a. Yamagishi, T. Haino, *Org. Lett.* **2014**, *16*, 2896-2899.

[3] Z. Peng, P.-P. Jia, X.-Q. Wang, X.-L. Zhao, H.-B. Yang, W. Wang, *CCS Chem.* **2024**, DOI: 10.31635/ccschem.024.202303738.